CALIFORNIA INSTITUTE OF TECHNOLOGY

EARTHQUAKE ENGINEERING RESEARCH LABORATORY

SEISMIC EARLY WARNING SYSTEMS: PROCEDURE FOR AUTOMATED DECISION MAKING

BY

VERONICA F. GRASSO, JAMES L. BECK AND GAETANO MANFREDI

REPORT NO. EERL 2005-02

PASADENA, CALIFORNIA

NOVEMBER 2005

Acknowledgments

We thank Hiroo Kanamori and Thomas Heaton of the California Institute of Technology who shared their experience and insights throughout the study reported here. The first author gratefully acknowledges the financial support from the University of Naples "Federico II" for her doctoral studies and while she was a Visiting Special Student at Caltech.

Seismic Early Warning Systems: Procedure for Automated Decision Making

V. Grasso[1], J. L. Beck[2], G. Manfredi[3]

[1]Department of Structural Analysis and Design, University of Naples, "Federico II";
Visiting Special Student, Caltech

[2]Department of Applied Mechanics and Civil Engineering, Caltech

[3]Department of Structural Analysis and Design, University of Naples, "Federico II"

Abstract

An Early Warning System potentially allows mitigation measures to be carried out from the moment in which a seismic event is detected. Examples of such measures are evacuation of buildings, shut-down of critical systems (nuclear reactors, industrial chemical processes, etc.) and stopping of high-speed trains. The type of mitigation measures that can be effectively activated depends on the amount of warning time available, but timeliness is often in conflict with the reliability of the predictions, which become more accurate as more seismic sensor data is collected. There is therefore an inevitable trade-off between the amount of warning time available and the reliability of the predictions provided by the Early Warning System. To investigate this trade-off, the consequences of the two alternatives of taking mitigation actions or not acting must be analyzed, accounting for significant uncertainty in the predictions.

In this report, we present a decision-making procedure based on the real-time evaluation of the consequences of taking no action and of activating mitigation measures which is based on the probabilities of false and missed alerts. The threshold at which mitigating actions should be taken is quantified based on a cost-benefit analysis. The method is applied to two recent seismic events in Southern California, an M 4.75 event in Yorba Linda and an M 6.5 event in San Simeon. Also, a feasibility assessment of any proposed regional Early Warning System is of critical importance, and it should involve an examination of whether the requirements, in terms of warning time available and the probability of making wrong decisions, are met. A useful tool in this assessment of an Early Warning System is a seismic hazard map to provide the probability of exceedance of ground shaking intensity, given a site and time interval of interest, and a corresponding map of the probability of making a wrong decision. In this report, a methodology is presented for estimating the probabilities of making wrong decisions that can be incorporated in a feasibility assessment of proposed Early Warning System.

Contents

Figures

1. Introduction

The high social and economic vulnerability of urbanized areas to seismic risk has become evident in recent years due to severe losses as a consequence of catastrophic earthquakes. The extent of structural damage and economic loss due to these catastrophic events underlines the strong necessity of social, political and scientific cooperation for disaster prevention.

It is clear that timely warnings can mitigate the effects of natural disasters. Such warnings are commonly given for floods, hurricanes, tornados and tsunamis, but still under development for earthquakes. Effective early warning technologies for earthquakes are much more challenging to develop because warning times range from only a few seconds to a minute or so (Allen and Kanamori, 2003). In areas close to faults, where seismic early warning systems (EWS) represent a mandatory necessity, only tens of seconds of warning are available. Such short warning times mean that to be effective a seismic EWS must depend on automated procedures, including those for decision making about whether to activate mitigation measures; the time is too short to require human intervention when the event is first detected. As a result of the automation, careful attention must be paid to the design of the local seismic EWS for each critical facility; in particular, a means of controlling the trade-off between false alarms and missed alarms is desirable.

Of course, as an essential part of a seismic EWS, an infrastructure must be in place that consists of a seismic sensor network with high-speed communication to some data-processing center, along with a broadcasting system to disseminate the early warning information to the local automated system that can activate the mitigation measures designed for a specific facility.

Historical lessons come of some help to appreciate the EWS potentialities. In the Indian

Ocean tsunami disaster of 26 December 2004, a tsunami EWS was in place for the Pacific Ocean that detected the large Sumatran subduction zone event but there was an inadequate broadcasting system to disseminate the early warning information to the countries at risk surrounding the Indian Ocean. Many thousands of lives could have been saved if a preventive alarm had been broadcasted to warn people in the coastal regions about the tsunami. In this case, for those locations sufficiently far from the ruptured segment of the Sumatran subduction zone, warning times of several hours were possible, so that before the tsunami arrived, many people might have been able to escape from the low-lying coastal areas to higher elevations. This mitigation action would have been enhanced by the availability of predicted inundation and damage maps to direct people to safer locations.

Although early warning technologies have been developed to provide natural hazard mitigation for many types of hazards, attention here is focused on seismic risk mitigation because the technologies for this application are not yet fully developed.

1.1. Potential benefits of seismic Early Warning Systems

The main goal of an EWS for earthquakes is the reduction or prevention of loss of life and mitigation of structural damage and economic loss. The benefits of EWS are due to the measures that can be carried out from the moment in which a seismic event is detected at a certain place until the moment in which the seismic waves arrive at a location of interest. These measures, for prevention or emergency response, can be categorized by considering the phases of the seismic event (Wieland, 2001).

After event detection but before the earthquake arrives at a site, the warning provided by EWS with pre-arrival times of up to perhaps 90 seconds, could be used to evacuate buildings, shut-down critical systems (such as nuclear and chemical reactors), put vulnerable machines and industrial robots into a safe position, stop high-speed trains, activate structural control systems

(Kanda et al. 1994, Occhiuzzi et al. 2004), and so on.

During an earthquake, the alarm generated by EWS could still enable such mitigation processes to be activated if there was insufficient time to do so prior to the arrival of the earthquake at the site. Within seconds after an earthquake, the information provided by EWS could be used to produce damage and loss maps based on the ground shaking intensity and could be the basis for more effective emergency response and rescue operations.

Evacuation of at-risk buildings and facilities is only feasible if the warning time is around 1 minute before the arrival of the strong shaking, which is possible only in the case where the seismic source zone is sufficiently far away. This is the situation, for example, for the threat to Mexico City from earthquakes occurring in the subduction zone along the Pacific Coast (e.g. Lee and Espinosa-Aranda, 1998), where the time available is sufficient to alert large segments of the population by commercial radio and television, and for evacuation of strategic buildings, such as schools, crowded facilities, and so on.

In the case of a few seconds warning time before the shaking, it is still possible to slow down trains (e.g. Saita and Nakamura, 1998), to switch traffic lights to red (as for the Lions Gate bridge EWS, Vancouver), to close valves in gas and oil pipelines, to release control rods in nuclear power plants (e.g. Wieland *et al*., 2000), activate structural control systems, and so on. In addition, secondary hazards can be mitigated that are triggered by earthquakes but which take more time to develop, such as landslides, tsunamis, fires, etc., by predicting the ground motion parameters for the incoming seismic waves. This could be used, for example, to initiate the evacuation of endangered areas.

Given that an appropriate EWS is in place for a local area or critical facility, its impact or effectiveness is dependent on the warning time available and the quality and reliability of the

information that is provided, since these influence and constrain the utilization of the information. In most EWS applications, the available warning time is likely to be no more than tens of seconds, enabling the possibility of activating mitigation measures but meaning that automated activation is essential to fully utilize the available warning time.

1.2. Limitations of effectiveness of seismic Early Warning Systems

The benefits of an EWS for earthquakes are often not fulfilled due to limitations that depend on:

1. the amount of warning time
2. the probability of making wrong decisions (false alarms and missed alarms)

These parameters strongly influence EWS impact and effectiveness on seismic risk reduction. Each of these is discussed in turn.

To examine the available warning time for activation of seismic mitigation measures, the main principle on which an EWS is based is first described. This principle is that seismic waves travel through the Earth with a velocity that is much less than the velocity of the electromagnetic signals transmitted by telephone or radio to provide seismic information about the incoming event. In addition, seismic body waves can be identified as compression waves (primary waves or P-waves) and shear waves (secondary waves or S-waves) (Occhiuzzi *et al*., 2004), where the P-waves are characterized by a propagation velocity that is almost twice that of S-waves; the latter are stronger and give almost horizontal ground motion at the base of a structure, in contrast to P-waves, so S-waves tend to be more damaging. The time interval from the detection of P-waves in the epicentral area, and the arrival of S-waves in the area where the structure or facility is located, may be utilized to activate mitigation measures. The feasible warning time is given by:

$$T_w = T_s - T_r \quad (1)$$

$$T_r = T_d + T_{pr} \quad (2)$$

where the origin of time is the P-wave detection time; T_r is the reporting time comprised of the time T_d needed by the system to trigger and record a sufficient length of waveforms and the time T_{pr} to process the data; T_s is the S-wave travel time and T_w is the early warning time. For the warning time to be considered adequate for the activation of a mitigation measure, it has to be greater than the time necessary for activation of the measure.

Suppose that the EWS works by setting an alarm if a critical shaking intensity threshold is predicted to be exceeded at a site, where the choice of critical threshold depends on the vulnerability of the system to be protected at the site. Assuming that the warning time provided by the EWS is sufficient for activation of the mitigation measure, then based on the predictions from the first few seconds of P-wave observation, a decision has to be made of whether to activate the alarm or not. In making this decision, two kinds of errors may be committed (Wald, 1947):

Type I error: the alarm is not activated when it should have been.

Type II error: the alarm is activated when it should not have been.

We call Type I errors *missed alarms* and type II errors *false alarms*. The probability of each of these wrong decisions is denoted by:

P_{ma}= probability of missed alarm, that is, the probability of having critical threshold exceedance but no alarm activation.

P_{fa} = probability of false alarm, that is, the probability of having no threshold exceedance but alarm activation.

The tolerance of a type I or II error is related to a trade-off between the benefits of a correct decision and the costs of a wrong decision and it could vary substantially, depending on the relative consequences of possible missed and false alarms. For example, the automated opening of a fire

station door has minimal impact if the door is opened for a false alarm. On the contrary, an automated shutdown of a power plant because of a false alarm could cause problems over an entire city and involve expensive procedures to restore to full-operational status. In this latter case, the EWS must be designed to keep the frequency of false alarms very low. In general, the automated decision process has to be designed with attention focused on the probability of false and missed alarms along with a cost-benefit analysis. Some mitigation measures could be unacceptable to operate as a result of the false or missed alarm rate being too high.

The probability of a wrong decision is due to having only partial knowledge of the phenomenon and so any prediction, as a consequence, is affected by uncertainty. A key element of an EWS is a better understanding of the parameters that play a fundamental role in this uncertainty, and hence a better understanding of the quality of the predictions on which decision making is based.

2. Ground motion prediction process in seismic EWS

2.1. Basic idea of EWS operation

The EWS is composed of a network of seismic stations, a dedicated real-time data communication system, central processing system, broadcasting system and information receivers at the user's end. In some cases, this network may be a dedicated local one placed at some distance around a structure to provide data about incoming seismic waves. When a seismic event occurs, the stations close to the epicentral area are triggered by P-waves, then the ground motion data is recorded and sent by the communication system to the central processor, where, based on predictive models, an evaluation is made in real-time to predict the earthquake source parameters of the event.

This information is provided to the user by a distribution network, and based on this early

information, the user predicts a ground motion or structural performance parameter of interest for a facility. This parameter represents the predictor on which the decision whether to raise the alarm or not is based. In this report, the predictor is taken to be an intensity measure *IM*, which is a ground motion parameter that represents the shaking intensity at the site of the facility. Two common intensity measures are peak ground acceleration (PGA) and response spectral acceleration (S_a). The *IM* is to be predicted based on the first few seconds of data registered by some of the seismic stations in a regional network that are near the earthquake source. The parameter of interest for a facility could also be taken as some critical engineering demand parameter, such as inter-story drift in a building or floor acceleration at the location of vulnerable equipment, or even economic loss.

The prediction model for the ground motion parameters can be represented as a sequential multi-compartment model (Bates *et al*., 2003), composed of two sub-models, M_1 and M_2 (Grasso *et al*., 2005), as illustrated in Figure 1.

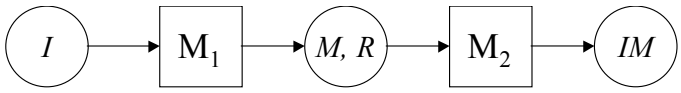

Figure 1. The multi-component model representing EWS.
M_1 is the earthquake prediction model and M_2 is the ground motion attenuation model

The earthquake prediction model, M_1, estimates earthquake source parameters (magnitude, *M*; epicentral distance, *R*), based on parameters, *I*, extracted from real-time measurements of the first few seconds of P-waves, e.g., *I* is the predominant period in Allen and Kanamori (2003); while *I* is the observed ground motion ratio for the Virtual Seismologist method in Cua and Heaton (2004).

The ground motion attenuation model, M_2, predicts ground motion parameters (intensity

measures *IM*), based on the magnitude and epicentral distance predicted by M_1. The parameter *IM*, which could be the final outcome of the EWS prediction process, represents the predicted ground motion intensity (e.g. PGA, PGV or S_a) that will occur at the site where a strategic facility of interest is located. It is assumed in this work that *IM* is the predictor on which the decision to take some protective action is based.

2.2. Sources of uncertainty

Uncertainty in the predictor *IM* is a result of the uncertain prediction errors produced by the models M_1 and M_2. The uncertainties for each model are represented in Figure 2, where ε_M, ε_R and ε_{IM} denote the prediction errors for the magnitude and location and the attenuation model, respectively. Uncertainties of each sub-model propagate through the output, so each uncertainty plays an important role in the definition of the final quality of the intensity measure, *IM*.

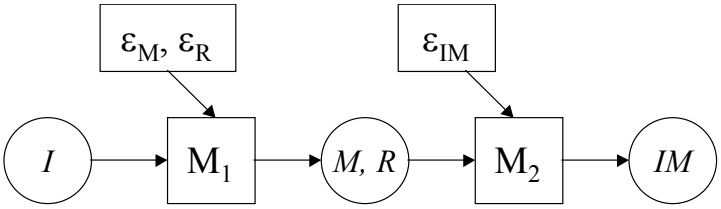

Figure 2. The multi-component model for EWS uncertainty propagation.

A Gaussian probability distribution model is chosen for ε_M and ε_{IM} to model the magnitude and attenuation model uncertainties. The uncertainty in the predicted magnitude can be well modeled as a Gaussian distribution, as shown by Cua and Heaton (2004), with standard deviation dependent on the prediction model. The magnitude error has zero-mean and a standard deviation of about 0.4 magnitude units for the Heaton-Cua relation and it decreases with increasing number of

data. According to the Allen-Kanamori method, the uncertainty of magnitude prediction is related to the number of stations considered and to the elapsed time, and it assumes a value of 0.7 magnitude units considering only one station, 0.6 for three stations, 0.45 for five stations, and it drops to 0.35 if ten stations are considered (Allen 2003). The errors related to the ground motion parameter conditional on *M* and *R* being given are modeled well by a lognormal distribution, so if the intensity measure *IM* is the logarithm of the ground motion parameter, then *IM* can be assumed to be Gaussian. This assumption is supported by the analysis done by Cua and Heaton (2004) in which the errors were analyzed based on a large number of data from ground motions recorded by the seismic network in Southern California over 4 years.

In this work, the uncertainty $\varepsilon_{\log R}$ in the natural logarithm $\log_e R$ of the epicentral distance prediction is modeled as Gaussian, which means that *R* has a lognormal distribution. It also means that for small prediction errors, $\varepsilon_R \approx \hat{R}\varepsilon_{\log R}$ is approximately Gaussian. It has been suggested that a more complex distribution for ε_R might be appropriate based on the observation that in the case of large-magnitude teleseismic events, the probability of a large prediction error based on the first few seconds of data is likely; in fact, in this case, the network could erroneously locate the epicenter inside the instrumented area (Kanamori and Heaton 2004, personal communication).

2.3. Uncertainty propagation

The quality of the predictions for the ground motion parameter of interest is fundamental for optimization of the decision-making process. This quality is influenced by the errors of the sub-models that propagate through to the output and influence the effectiveness of the EWS application. In particular, it is necessary to estimate the total prediction error in order to quantify the performance of the EWS prediction process in terms of the probability of false and missed alarms.

For this purpose, all the prediction errors influencing the intensity measure have to be considered, as shown in Figure 2, along with their corresponding probability distributions.

The total prediction error is given by comparing the predicted intensity measure, $I\hat{M}$, to the actual *IM*:

$$\varepsilon_{tot} = IM - I\hat{M} \tag{3}$$

where $I\hat{M}$ is a function of the predicted values $\hat{M}$ and $\hat{R}$, which can be expressed in terms of the actual M and R and the uncertain prediction errors ε_M and $\varepsilon_{\log R}$:

$$I\hat{M} = f(\hat{M}, \log_e \hat{R}) = f(M - \varepsilon_M, \log_e R - \varepsilon_{\log R}) \tag{4}$$

where the function f represents the ground motion attenuation model as follows:

$$f(M, \log_e R) = \alpha + \beta M + \gamma \log_e R \tag{5}$$

Most published attenuation models have this form if *IM* denotes $\log_e$ PGA or $\log_e S_a$ (Seismological Research Letters, 1997); in the examples later, *IM* is taken to be $\log_e$ PGA. The actual intensity measure, *IM*, is represented by:

$$IM = f(M, \log_e R) + \varepsilon_{IM} \tag{6}$$

where ε_{IM} is the prediction error in the ground motion attenuation model, given *M* and *R*.

Under previous assumptions about ε_M, $\varepsilon_{\log R}$ and ε_{IM}, the total prediction error ε_{tot} also follows a Gaussian distribution with a mean and variance that depends on the means and variances of these contributing prediction errors, since:

$$\begin{aligned} \varepsilon_{tot} &= IM - I\hat{M} = f(M, \log_e R) + \varepsilon_{IM} - f(M - \varepsilon_M, \log_e R - \varepsilon_{\log R}) \\ &= \beta\varepsilon_M + \gamma\varepsilon_{\log R} + \varepsilon_{IM} \\ &\approx \beta\varepsilon_M + \frac{\gamma}{\hat{R}}\varepsilon_R + \varepsilon_{IM} \end{aligned} \tag{7}$$

Under the assumption of independence of errors, the variance of ε_{tot} is:

$$\sigma_{tot} = \sqrt{\beta^2\sigma_M^2 + \gamma^2\sigma_{\log R}^2 + \sigma_{IM}^2} \approx \sqrt{\beta^2\sigma_M^2 + \frac{\gamma^2}{\hat{R}^2}\sigma_R^2 + \sigma_{IM}^2} \quad (8)$$

and the mean of ε_{tot} is equal to:

$$\mu_{tot} = \beta\mu_M + \gamma\mu_{\log R} + \mu_{IM} \quad (9)$$

If the empirically-derived models M_1 and M_2 (Figures 1 and 2) are unbiased, then the mean $\mu_{tot} = 0$. In fact, μ_{tot} does have a value close to zero in the Virtual Seismologist method (Cua and Heaton 2004). If more complex attenuation models, or more complex probability models for ε_M, $\varepsilon_{\log R}$ and ε_{IM}, are used, this analytical approach may be not applicable and then a Monte Carlo method is suggested to quantify the uncertainty in ε_{tot} (see Appendix).

3. Probability of wrong decisions: pre-installation analysis

3.1. Probabilities of false and missed alarms: pre-installation analysis

When examining the feasibility of installing an EWS for a facility, it is important to have a mechanism to control the probabilities of false and missed alarms. Since the decision to activate the alarm is based on a predictor, $\hat{IM}$, false alarms can be caused by the predictor exceeding the warning threshold even though the actual intensity measure, *IM*, that occurs at the site does not reach the critical value. Similarly, missed alarms can be caused by the predictor not exceeding the warning threshold even though the actual intensity measure reaches its critical value.

For a given facility, the critical threshold, *a*, of *IM* must be chosen by the user based on a vulnerability analysis of the system to be protected; for example, it could be chosen as the value of *IM* for which there is a high probability that damage (or significant economic losses) will occur. To

control the probability of wrong decisions, the warning threshold is chosen as the product of the critical threshold a and a parameter, c, to be specified during the design process. The critical threshold depends on the facility, structure or equipment to be protected, but the warning threshold $c \cdot a$ depends on the design process chosen to optimize the automated alarm activation system. The design parameter c provides a mechanism to control the incidence of false and missed alarms. It is not possible to simultaneously reduce both of these but the design parameter c can be used to control the trade-off between them.

A false alarm occurs when the EWS predicts a value, $\hat{IM}$, that exceeds the warning threshold, $c \cdot a$, while the actual value, IM, of the intensity measure at the site turns out to be less than the value of the critical threshold, a. For a pre-installation analysis, the probability of a false alarm is therefore given by:

$$P_{fa} = \mathrm{P}[IM \le a \mid \hat{IM} > c \cdot a] \tag{10}$$

Similarly, the probability of a missed alarm is given by:

$$P_{ma} = \mathrm{P}[IM > a \mid \hat{IM} \le c \cdot a] \tag{11}$$

The values of the probabilities of false and missed alarms, P_{fa} and P_{ma}, are an important tool for the decision-making process during pre-installation design and during operation in a seismic event.

During design, the anticipated rate of missed and false alarms represents a guideline for EWS feasibility. The realization of EWS could be feasible or not, depending on whether the requirements in terms of warning time available and the probability of wrong decisions can be met. A useful tool to evaluate an EWS may be constructed by using a seismic hazard map to provide the probability of exceedance of ground shaking intensity, given a site and time interval of interest, to produce a map of probability of wrong decisions. Such a map would help when performing a territorial feasibility assessment of EWS applications.

During a seismic event, the (automated) decision to activate protective measures may be done either by comparing the requirements in terms of warning time needed and the tolerable level of P_{fa} (or P_{ma}) based on the information made available by the EWS, or by monitoring a time-varying threshold $c(t)\cdot a$. This case is examined later in Section 5.

The main reason for evaluating the probability of wrong decisions using a pre-installation analysis is to design the warning threshold, which can be chosen based on the probabilities of false and missed alarms and their expected annual frequency that are tolerable to the owner or manager of the facility to be protected. By estimating the probability of false and missed alarms during design of the EWS application, we are primarily trying to answer to the question: How would an EWS perform during earthquakes that might occur in the area of interest, in terms of a false and missed alarm rates?

The probabilities of false and missed alarms in a pre-installation analysis are evaluated as a time-independent variable based on the seismicity of the area of interest. Time dependence can be neglected as a first approximation. A more refined analysis is presented later in Section 5 for the operation of an EWS application during a seismic event, where the changes in estimated magnitude and location coming from the EWS are taken into account. In any case, the prediction uncertainty stabilizes after some time following the first triggering. In some special cases, such as Mexico City, the location of the fault area and the configuration of the seismic stations lead to stabilization of the uncertainty of the prediction after the first few seconds.

3.2. Prior information: hazard function

Prior information can be expressed by using the hazard (rate) function (Kramer 1996) that gives the mean annual rate of events with intensity measure exceeding a certain critical value, given

a site of interest. The hazard function for a site comes from a PSHA (probabilistic seismic hazard analysis). It directly provides information related to the expected frequency of occurrence of the intensity measure *IM* for a given site and time period of interest; on the other hand, the EWS gives the predicted intensity measure, $\hat{IM}$, that differs from the actual *IM* by the prediction error, ε_{tot}. This error depends on the errors related to the prediction of magnitude, *M*, and epicentral distance, *R*, and the prediction error of the ground motion attenuation model. Figure 3 shows the relation between *IM* and $\hat{IM}$ given by ε_{tot}, which depends on ε_M, ε_R and ε_{IM} as in Eq. 7.

The goal of the analysis that follows is to describe the EWS behavior in terms of the probabilities of having false and missed alarms, based on a given seismic hazard environment represented by the intensity measure hazard function, $\lambda(IM)$. Considering all the possible events, the probability of a wrong decision is determined for a given site and a given period of time (e.g. one year). The key to forecasting the behaviour of the EWS is the prior knowledge about the errors that are committed when predicting the intensity measure. This prior knowledge comes from an analysis of the uncertainty propagation of the errors, as described in Section 2.

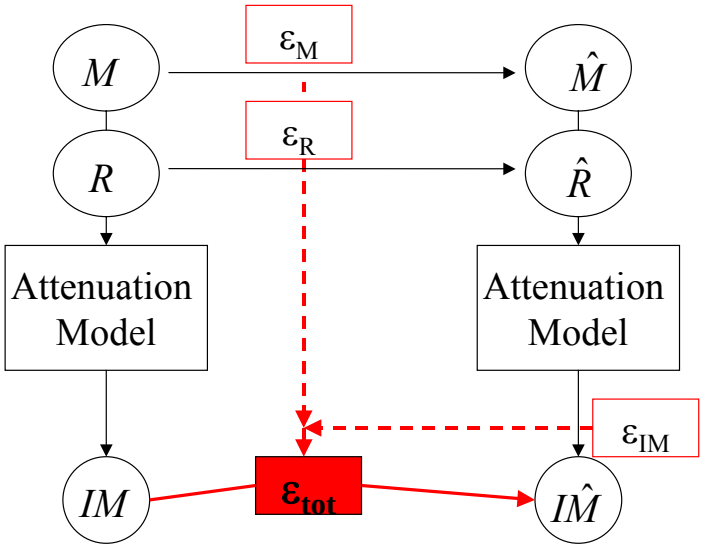

Figure 3. Simulation of the EWS process of prediction in a pre-installation analysis.

The hazard function defines the mean annual rate of exceedance of a critical value of the ground motion intensity measure; from this mean rate, the probability of exceedance of a critical value, given that an earthquake of interest has occurred, can be determined as follows, which is based on a Poisson process model for the temporal occurrence of earthquakes:

$$\lambda(IM_c) = \lambda(IM_0) \cdot P[IM > IM_c \mid IM > IM_0] \tag{12}$$

where IM_0 is the minimum value of the intensity measure that is of interest (cut-off value) and it is used to define the earthquakes of interest.

An exponential model is assumed for the hazard function for a site (but recall that the choice of IM used in the examples is $\log_e$ PGA so this corresponds to a power law on PGA):

$$\lambda(IM) = k_0 10^{-k_1 IM} \tag{13}$$

where k_0 and k_1 can be obtained by fitting the hazard function from a PSHA for the site. This model implies from Eq. 12 that:

$$P\left[IM > IM_c \mid IM > IM_0\right] = 10^{-k_1(IM_c - IM_0)} \tag{14}$$

The cumulative distribution function is then:

$$P\left[IM \le IM_c \mid IM > IM_0\right] = 1 - 10^{-k_1(IM_c - IM_0)} \tag{15}$$

and the expression for the PDF (probability density function) is derived by differentiating this cumulative distribution function:

$$p\left(IM \mid IM > IM_0\right) = k_1 \cdot \log_e 10 \cdot 10^{-k_1(IM - IM_0)} = \overline{c} \cdot 10^{-k_1 IM} \tag{16}$$

where $\overline{c} = k_1 \cdot \log_e 10 \cdot 10^{k_1 IM_0}$.

In this work, the parameter k_1 is estimated from a hazard function for the site of interest by using a minimum entropy criterion in which the relative entropy E is minimized with respect to k_1:

$$E = \sum_i p_i \log\left(\frac{p_i}{q_i}\right) \tag{17}$$

where p_i represents the discrete probability distribution function derived from $p\left(IM \mid IM > IM_0\right)$ and q_i is the discrete probability distribution function derived from the given hazard function $\lambda(IM)$ using Eq. 12, so q_i is obtained by numerically differentiating the cumulative distribution function in the same way as $p\left(IM \mid IM > IM_0\right)$ was derived above. Therefore, p_i is a function of the parameter k_1 but q_i is not. By minimizing the relative entropy, we determine the parameter k_1 so that the model PDF is the best fit in an information-theoretic sense to the PDF implied by the hazard function for the site.

3.3. Probability of false alarm: pre-installation analysis

The probability of false alarms, as defined in Eq. 10, can be expressed using Bayes rule as:

$$\begin{aligned} P_{fa} &= P\left[IM \le a \mid \hat{IM} > c \cdot a, IM > IM_0 \right] \\ &= \frac{P\left[IM \le a \cap \hat{IM} > c \cdot a \mid IM > IM_0 \right]}{P\left[\hat{IM} > c \cdot a \mid IM > IM_0 \right]} \end{aligned} \tag{18}$$

where it is assumed that an earthquake of interest, i.e. $IM > IM_0$, has occurred and that $a > IM_0$.

The numerator, let us call it $P_{fa,1}$, is evaluated as:

$$\begin{aligned} P_{fa,1} &= P\left[IM \le a \cap \hat{IM} > c \cdot a \mid IM > IM_0 \right] \\ &= \int_{ca}^{\infty} \int_{IM_0}^{a} p(IM, \hat{IM} \mid IM > IM_0) dIM d\hat{IM} \end{aligned} \tag{19}$$

which can be written, using Bayes rule, as:

$$P_{fa,1} = \int_{IM_0}^{a} \int_{ca}^{\infty} p(\hat{IM} \mid IM) \cdot p(IM \mid IM > IM_0) d\hat{IM} dIM \tag{20}$$

where $p\left(IM \mid IM > IM_0\right)$ is given by Eq. 16 and $p(\hat{IM} \mid IM)$ is a Gaussian distribution with IM representing the mean value (if ε_{tot} has zero mean) and standard deviation σ_{tot} given by Eq. 8. In the case that the prediction, $\hat{IM}$, is affected by a significant bias error (i.e. mean μ_{tot} of ε_{tot} is not close

to zero), then the mean of the Gaussian distribution $p(I\hat{M} \mid IM)$ is (IM - μ_{tot}) (see Eq. 3). Substituting in Eq. 20:

$$P_{fa,1} = \int_{IM_0}^{a} \int_{ca}^{\infty} \frac{1}{\sigma_{tot}\sqrt{2\pi}} \exp\left[-\frac{1}{2}\left(\frac{I\hat{M} - IM}{\sigma_{tot}} \right)^2 \right] \cdot \overline{c} \cdot 10^{-k_1 IM}\, dI\hat{M} dIM \tag{21}$$

The integral of the Gaussian distribution over $I\hat{M}$ can be expressed in terms of the standard Gaussian cumulative distribution function Φ:

$$\int_{ca}^{\infty} \frac{1}{\sigma_{tot}\sqrt{2\pi}} \exp\left[-\frac{1}{2}\left(\frac{I\hat{M} - IM}{\sigma_{tot}} \right)^2 \right] dI\hat{M} = \Phi\left(-\frac{ca - IM}{\sigma_{tot}} \right) \tag{22}$$

so Eq. 21 can be cast in a simpler form:

$$P_{fa,1} = \int_{IM_0}^{a} \Phi\left(-\frac{ca - IM}{\sigma_{tot}} \right) \cdot \overline{c} \cdot 10^{-k_1 IM}\, dIM \tag{23}$$

The denominator of P_{fa} in Eq. 18 is expressed as:

$$P_{fa,2} = \int_{ca}^{\infty} p(I\hat{M} \mid IM > IM_0) dI\hat{M} \tag{24}$$

which can be written, using the theorem of total probability, as:

$$P_{fa,2} = \int_{IM_0}^{\infty} \int_{ca}^{\infty} p(I\hat{M} \mid IM) \cdot p(IM \mid IM > IM_0) dI\hat{M} dIM \tag{25}$$

This can be expressed in terms of the standard Gaussian cumulative distribution function Φ as:

$$P_{fa,2} = \int_{IM_0}^{\infty} \Phi\left(-\frac{ca - IM}{\sigma_{tot}} \right) \cdot \overline{c} \cdot 10^{-k_1 IM}\, dIM \tag{26}$$

Summarizing, the probability of false alarm in a pre-installation analysis is given by:

$$P_{fa} = \frac{\int_{IM_0}^{a} \Phi\left(-\frac{ca - IM}{\sigma_{tot}} \right) \cdot 10^{-k_1 IM}\, dIM}{\int_{IM_0}^{\infty} \Phi\left(-\frac{ca - IM}{\sigma_{tot}} \right) \cdot 10^{-k_1 IM}\, dIM} \tag{27}$$

The integrals in the denominator and numerator here can be evaluated numerically for different

values of c, given the value of a; then curves of P_{fa} versus c can be plotted for different critical thresholds a. Examples are given later in Section 6.

3.4. Probability of missed alarm: pre-installation analysis

The probability of missed alarms, as defined in Eq. 11, can be written using Bayes rule as:

$$P_{ma} = P\left[IM > a \mid I\hat{M} \le c \cdot a, IM > IM_0 \right] = \frac{P\left[IM > a \cap I\hat{M} \le c \cdot a \mid IM > IM_0 \right]}{P\left[I\hat{M} \le c \cdot a \mid IM > IM_0 \right]} \tag{28}$$

where once again it is assumed that an earthquake of interest has occurred and that $a > IM_0$. The numerator can be expressed as:

$$\begin{aligned} P_{ma,1} &= P\left[IM > a \cap I\hat{M} \le c \cdot a \mid IM > IM_0 \right] \\ &= \int_{-\infty}^{ca} \int_{a}^{\infty} p(IM, I\hat{M} \mid IM > IM_0) dIM dI\hat{M} \end{aligned} \tag{29}$$

which can be written, using Bayes rule, as:

$$P_{ma,1} = \int_{a}^{\infty} \int_{-\infty}^{ca} p(I\hat{M} \mid IM) \cdot p(IM \mid IM > IM_0) dI\hat{M} dIM \tag{30}$$

where $p\left(IM \mid IM > IM_0\right)$ is given by Eq. 16 and $p(I\hat{M} \mid IM)$ is a Gaussian distribution as before (see after Eq. 20). Substituting in Eq. 30:

$$P_{ma,1} = \int_{a}^{\infty} \int_{-\infty}^{ca} \frac{1}{\sigma_{tot}\sqrt{2\pi}} \exp\left[-\frac{1}{2}\left(\frac{I\hat{M} - IM}{\sigma_{tot}} \right)^2 \right] \cdot \overline{c} \cdot 10^{-k_1 IM} \, dI\hat{M} dIM \tag{31}$$

The integral of the Gaussian distribution over $I\hat{M}$ can be expressed in terms of the standard Gaussian cumulative distribution function Φ:

$$\int_{-\infty}^{ca} \frac{1}{\sigma_{tot}\sqrt{2\pi}} \exp\left[-\frac{1}{2}\left(\frac{I\hat{M} - IM}{\sigma_{tot}} \right)^2 \right] dI\hat{M} = \Phi\left(\frac{ca - IM}{\sigma_{tot}} \right) \tag{32}$$

so Eq. 31 can be cast in a simpler form:

$$P_{ma,1} = \int_{a}^{\infty} \Phi\left(\frac{ca - IM}{\sigma_{tot}}\right) \cdot \overline{c} \cdot 10^{-k_1 IM}\, dIM \tag{33}$$

The denominator of P_{ma} in Eq. 28 is:

$$P_{ma,2} = \int_{-\infty}^{ca} p(I\hat{M} \mid IM > IM_0) dI\hat{M} \tag{34}$$

which can be expressed, using the theorem of total probability, as:

$$P_{ma,2} = \int_{IM_0}^{\infty} \int_{-\infty}^{ca} p(I\hat{M} \mid IM) \cdot p(IM \mid IM > IM_0) dI\hat{M} dIM \tag{35}$$

This can be expressed in terms of the standard Gaussian cumulative distribution function:

$$P_{ma,2} = \int_{IM_0}^{\infty} \Phi\left(\frac{ca - IM}{\sigma_{tot}}\right) \cdot \overline{c} \cdot 10^{-k_1 IM}\, dIM \tag{36}$$

The probability of missed alarms in a pre-installation analysis is therefore given by:

$$P_{ma} = \frac{\int_{a}^{\infty} \Phi\left(\frac{ca - IM}{\sigma_{tot}}\right) \cdot 10^{-k_1 IM}\, dIM}{\int_{IM_0}^{\infty} \Phi\left(\frac{ca - IM}{\sigma_{tot}}\right) \cdot 10^{-k_1 IM}\, dIM} \tag{37}$$

4. Threshold design and feasibility assessment

4.1. Designing the test procedure: alarm threshold setting

A test procedure leading to the acceptance or rejection of a hypothesis is simply a rule specifying whenever the hypothesis should be accepted or rejected based on the observed data. A test procedure can be defined by subdividing the sample space of all possible values that the predictor can assume into two exclusive regions (Wald, 1947):

- Region 1, for which acceptance of the hypothesis is preferred
- Region 2 is the critical region, for which rejection of the hypothesis is preferred

For EWS, the hypothesis of interest is the exceedance of the critical threshold of the intensity measure and Region 2 is represented by all the values of intensity measure for which the alarm should be activated and Region 1 where it should not to be activated. The critical region is defined by the critical threshold that is provided by the user, which could represent the likely occurrence of structural damage or heavy economic losses. On the other hand, the warning threshold corresponds to when the alarm should be raised. The warning threshold is defined by decision criteria based on the user's requirements, which could involve selecting tolerable levels for the probabilities of wrong decisions or be based on cost-benefit considerations. Both of these cases for warning threshold design are described and are analysed in this section. In Section 4.2, the criterion is related to a tolerable level of making wrong decisions, and in Section 4.3, to a cost-benefit analysis.

4.2. Threshold setting based on tolerated risks of making the wrong decision

In the case that the user's requirements are given as the tolerable values of probabilities of false and missed alarms, the test procedure can be designed as follows.

The goal is to design a test that satisfies the conditions imposed on P_{fa} (or P_{ma}) by controlling the alarm threshold c·a on $\hat{IM}$. If the probability of false alarms is lowered, then the probability of missed alarms is increased. To design the alarm threshold for *IM*, the trade-off between P_{fa} and P_{ma} must be studied. Because of this trade-off, there is a limit as to how much the probabilities of wrong decisions can be reduced. This limit can be studied by using Stein's lemma, which states:

If a large number *N* of observations is available, then as $P_{ma} \to 0,\ P_{fa} \to \exp\left[-N\ K(p_0, p_1)\right]$ where K is the relative entropy (Kullback-Leibler distance):

$$K(p_0, p_1) = \int p_1 \log_e \frac{p_1}{p_0} dIM \tag{38}$$

where p_0 is the PDF of IM conditioned on $\hat{IM} \le c \cdot a$ (null hypothesis) and p_1 is the PDF of IM conditioned on $\hat{IM} > c \cdot a$.

Based on the user's specifications of tolerable P_{ma}, the corresponding P_{fa} is given by Stein's Lemma. By means of the operating characteristic (OC) function, the warning threshold can be defined. The OC function represents the probability of acceptance of the null hypothesis which corresponds to the probability of no alarm activation.

The ideal test corresponds to the ideal OC function shown in Figure 4, which gives a probability of acceptance of 1 for $IM \le a$ when $\hat{IM} \le c \cdot a$ (in acceptance zone) and probability of acceptance of zero for $IM \le a$ when $\hat{IM} > c \cdot a$ (in the rejection zone). Note that the probability of acceptance conditioned on the predictor, $\hat{IM}$, may be written as $P\left[IM \le a \mid \hat{IM} \right]$, that corresponds to P_{fa} in the rejection (critical) zone and (1- P_{ma}) in the acceptance zone.

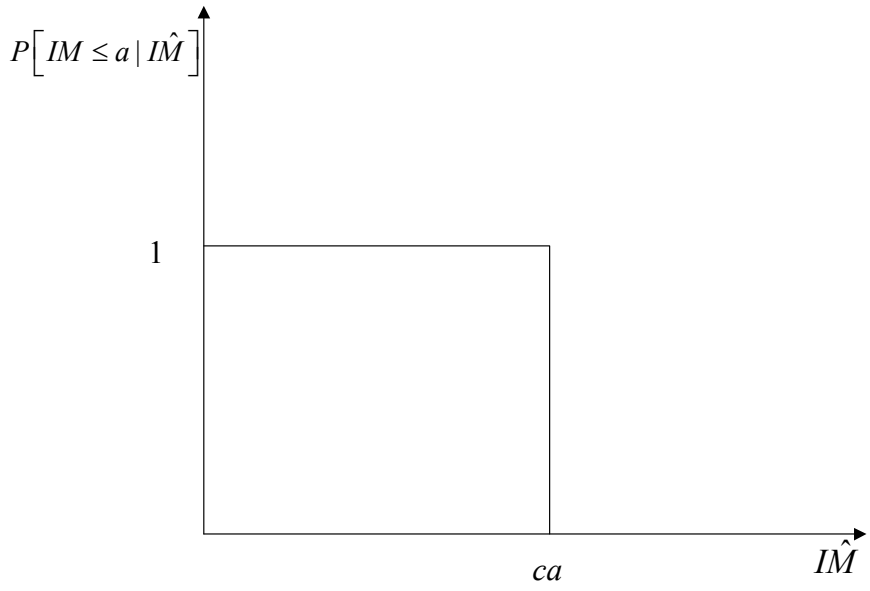

Figure 4. The ideal OC function

Based on uncertainties in the prediction of *IM* by $\hat{IM}$, which is based on the first seconds of observation of the seismic data, we cannot obtain an ideal OC function and we have to accept errors of type I and II (missed and false alarms). If the tolerable probability of a missed alarm in the acceptance zone is α and the tolerable probability of false alarm is β in the rejection zone, then the OC function will be characterized as in Figure 5 where β (or α) is the design requirement specified by the user and α (or β), respectively, is given by Stein's Lemma. The test is better designed if the OC function corresponding to the test is closer to the optimal OC function represented in Figure 5.

A prior definition of a possible set of thresholds, $c \cdot a$, can be defined and for each value of a the optimal OC function is defined. The discrete OC function representing the test may be evaluated at a finite number of points representative of the values of probabilities of wrong decisions for a range of values of $c \cdot a$ of interest. A best fitting curve can be constructed based on these points and the corresponding value of $c \cdot a$ will be the optimal warning threshold.

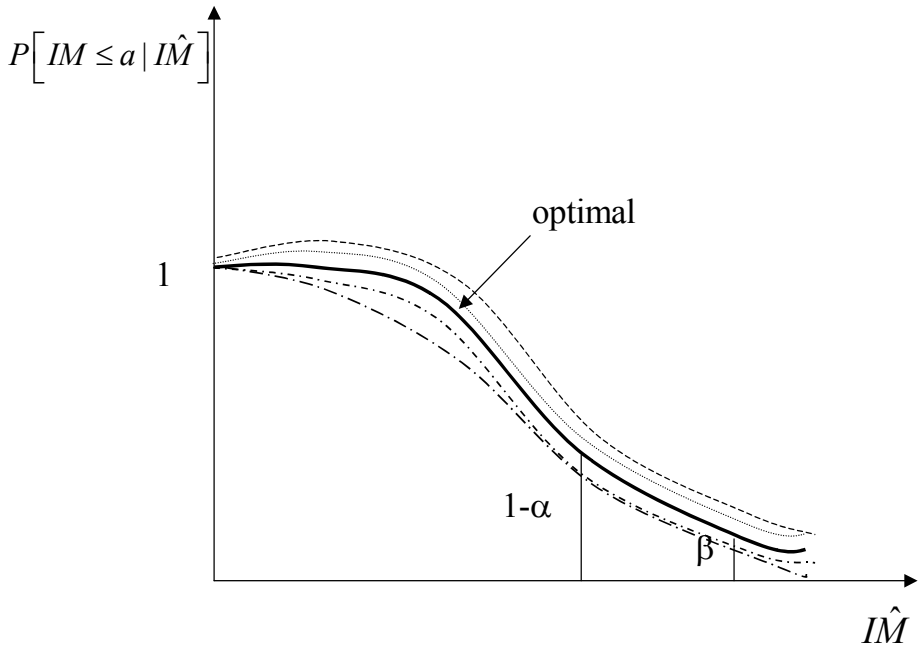

Figure 5. The optimal OC function

4.3. Threshold setting based on cost-benefit considerations

Instead of directly specifying tolerable probabilities of wrong decisions to represent the design parameters for setting the threshold, it may be more natural to derive them by examining the consequences of wrong decisions using a cost-benefit analysis. In this case, the decision criterion may be taken to be the minimization of the expected consequences over the two possible actions of raising the alarm or doing nothing. A cost benefit analysis is based on the details shown in Table 1.

Table 1. Cost benefit analysis for threshold design

Action	Cost for case: IM<a	Cost for case: IM>a
Raise Alarm	False alarm: C_{fa}	Good Alarm: C_{ga}
No Alarm	Good Missed Alarm: C_{gm}	Missed Alarm: C_{ma}

where:

$$C_{ga} = C_{eq} - C_{save} \qquad C_{ma} = C_{eq} \qquad C_{gm} \simeq 0$$
$$P_{ga} = 1 - P_{fa} \qquad P_{gm} = 1 - P_{ma} \tag{39}$$

Here, C_{eq} represents the expected costs due to the earthquake, C_{fa} is the cost of a false alarm and C_{save} is the expected savings as a consequence of the activation of the protective measure. If the alarm is raised, the expected cost is given by:

$$\begin{aligned} E\left[\text{cost} \mid \text{alarm}\right] &= C_{fa} \cdot P_{fa} + C_{ga} \cdot P_{ga} \\ &= C_{fa} \cdot P_{fa} + \left(C_{eq} - C_{save}\right) \cdot \left(1 - P_{fa}\right) \end{aligned} \tag{40}$$

On the other hand, if the alarm is not raised, the expected cost is given by:

$$\begin{aligned} E\left[\text{cost} \mid \text{no-alarm}\right] &= C_{gm} \cdot P_{gm} + C_{ma} \cdot P_{ma} \\ &= C_{ma} \cdot P_{ma} \end{aligned} \tag{41}$$

The decision criterion for deciding between the options, raising the alarm or not, is represented by the minimum cost rule: Raise the alarm if and only if

$$E\left[\text{cost} \mid \text{no-alarm}\right] \geq E\left[\text{cost} \mid \text{alarm}\right] \tag{42}$$

that is,

$$\begin{aligned} C_{eq} \cdot P_{ma} &\geq C_{fa} \cdot P_{fa} + (C_{eq} - C_{save}) \cdot (1 - P_{fa}) \\ &= (C_{save} + C_{fa} - C_{eq}) \cdot P_{fa} + (C_{eq} - C_{save}) \end{aligned} \tag{43}$$

Since the probabilities of false and missed alarms, P_{fa} and P_{ma}, are given by Eq. 27 and 37, respectively, and so may be evaluated as a function of the warning threshold parameter c, Eq. 43 can be taken as an equality to select an appropriate value of c. The tolerable value of P_{fa} and P_{ma} may then be determined from Eq. 27 and 37 for this value of c.

The above approach assumes that σ_{tot} in Eq. 27 and 37 is time invariant so that the alarm threshold value $c \cdot a$ for $\hat{IM}$ can be set prior to operation of the EWS, where the value of critical

threshold, a, is specified by the user. During a seismic event, however, more and more information becomes available to the EWS and so σ_{tot} will decrease with time. A refined analysis using a time-dependent warning threshold, $c(t)a$, would then be more appropriate. Alternatively, the probability of false and missed alarms could be monitored as a function of time and then the alarm would be raised when the tolerable level of probability of $P_{fa}(t)$ or $P_{ma}(t)$ is exceeded.

In the next section, we consider a refined decision-making procedure that is appropriate during a seismic event and which takes into account that the quality of the *IM* prediction improves as more and more information is obtained by the EWS. It is shown in section 5.1 that in this case: $P_{fa}(t) + P_{ma}(t) = 1$, so Eq. 43 implies that the probability of a false alarm is tolerable if and only if:

$$P_{fa}(t) \le \beta = \frac{C_{save}}{C_{fa} + C_{save}} \tag{44}$$

Similarly, since the alarm is not raised if and only if:

$$C_{eq} \cdot P_{ma} < (C_{save} + C_{fa} - C_{eq}) \cdot P_{fa} + (C_{eq} - C_{save}) \tag{45}$$

it follows that the probability of a missed alarm is tolerable if and only if:

$$P_{ma}(t) < \alpha = \frac{C_{fa}}{C_{fa} + C_{save}} \tag{46}$$

It is clear from Eq. 44 and 46 that in this case, where the decision criterion is based on a cost-benefit analysis, $\alpha + \beta = 1$, which directly exhibits the trade-off between the threshold probabilities that are tolerable for false and missed alarms. If the threshold β is reduced to make false alarms less likely, then the threshold α for missed alarms becomes correspondingly larger.

5. Decision making in EWS during a seismic event

5.1. Real-time uncertainty analysis during an event

During a seismic event, the probability of false and missed alarms will be updated with time as more stations are triggered by the seismic waves and more data comes in from those that have already been triggered. This increase in data available will produce a decrease with time in the uncertainty in the predicted earthquake location and magnitude. Therefore, the prediction of the intensity measure can be updated with time and the characterization of its uncertainty, σ_{tot} (t), will vary with time. As a consequence, it is important to update the probability of false and missed alarms as the seismic event evolves.

Recall that the predicted intensity measure, $\hat{IM}$, is estimated from the attenuation model based on the predictions of earthquake magnitude and location provided by EWS and so it can be updated as a function of time during the event. On the other hand, the actual intensity measure value, *IM*, that will occur at the site is unknown. The predicted and actual values of the intensity measure differ by ε_{tot}(t) as in Eq. 3:

$$IM = \hat{IM}(t) + \varepsilon_{tot}(t) \tag{47}$$

As shown in Figure 6, the total error ε_{tot}(t) is related to ε_M(t), ε_R(t) and ε_{IM}, which can be continually updated as additional information becomes available by using Bayesian updating, as in the Virtual Seismologist method (Cua and Heaton 2004). Given the predicted value of $\hat{IM}$ at time *t*, the uncertainty in *IM* can be modeled by a Gaussian distribution with mean equal to the prediction $\hat{IM}(t)$ and standard deviation equal to σ_{tot}(t), which can be evaluated by an analysis of the uncertainty propagation of the error, as was done to derive Eq. 8.

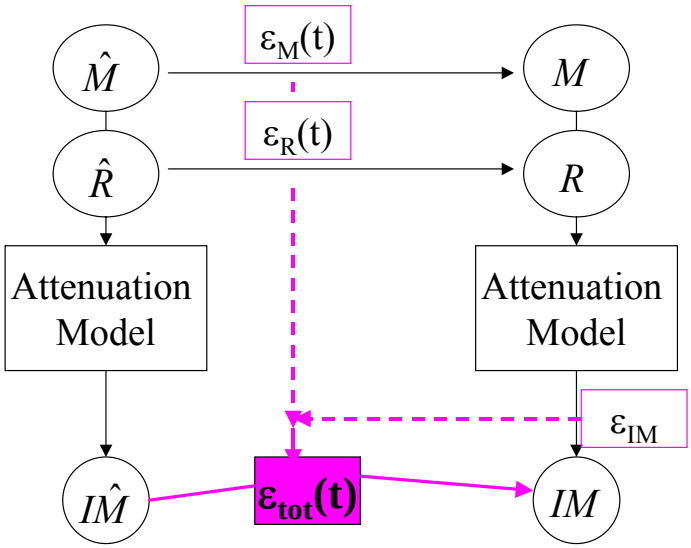

Figure 6. Simulation of the EWS prediction process, during the seismic event.

The potential probability of a false alarm is estimated as the probability of *IM* being less than the critical threshold, *a*, given the predicted value $\hat{IM}(t)$ (if the alarm is raised, it becomes an actual probability of false alarm):

$$P_{fa}(t) = \mathrm{P}[IM \le a \mid \hat{IM}(t)] \tag{48}$$

Since the uncertainty in *IM* is modeled as a Gaussian distribution with mean equal to the predicted $\hat{IM}(t)$ (if there is a known bias in the prediction, it should be added to this mean) and with standard deviation $\sigma_{tot}(t)$, evaluated as a function of the updated uncertainties for the earthquake magnitude and location, it follows that:

$$P_{fa}(t) = \int_{-\infty}^{a} \frac{1}{\sigma_{tot}(t)\sqrt{2\pi}} \exp\left[\frac{-(IM-\hat{IM}(t))^2}{2\sigma_{tot}(t)^2}\right] dIM = \Phi\left(\frac{a - \hat{IM}(t)}{\sigma_{tot}(t)}\right) \tag{49}$$

where Φ is the standard Gaussian cumulative distribution function. The potential probability of a missed alarm is equal to the probability of *IM* being greater than the critical threshold (if the alarm is not raised, it becomes the probability of a missed alarm):

$$P_{ma}(t) = \mathrm{P}[IM > a \mid \hat{IM}(t)] \tag{50}$$

and

$$P_{ma}(t) = \int_{a}^{\infty} \frac{1}{\sigma_{tot}(t)\sqrt{2\pi}} \exp\left[\frac{-(IM - \hat{IM}(t))^2}{2\sigma_{tot}(t)^2}\right] dIM = 1 - \Phi\left(\frac{a - \hat{IM}(t)}{\sigma_{tot}(t)}\right) \tag{51}$$

Since the two conditions ($IM \le a$ and $IM > a$) are mutually exclusive and exhaustive, the probabilities $P_{fa}(t)$ and $P_{ma}(t)$ always sum to one.

5.2. Decision making during the seismic event

The potential probabilities of false and missed alarms in Eq. 49 and 51 provide fundamental guidelines for the user's decision making during the seismic event, since they quantify the reliability of the information provided by the EWS. While the event is occurring, the decision to raise the alarm can be based on real-time monitoring of the probability of wrong decisions, focusing on the situation (false alarm or missed alarm) that the user is more concerned about. It will be demonstrated in this section that this can be done by monitoring whether the predicted intensity measure exceeds a time-varying warning threshold, $c(t)$ a.

The proposed procedure is as follows. Using Eq. 49 and 51, the value of the probabilities $P_{fa}(t)$ and $P_{ma}(t)$ are evaluated as time goes by during an event and they are compared to the tolerable values, which may be established based on cost-benefit considerations (see the end of Section 4.3). The alarm is raised when either $P_{fa}(t)$ or $P_{ma}(t)$ reaches its tolerable value, β and α, respectively, as shown in Figure 7. This assumes that the time available is sufficient for activation of the protective measures. If the time available reaches the minimum time necessary for activation of the protective measure, the alarm will be raised only if the probability of a wrong decision, evaluated at that time, can be accepted.

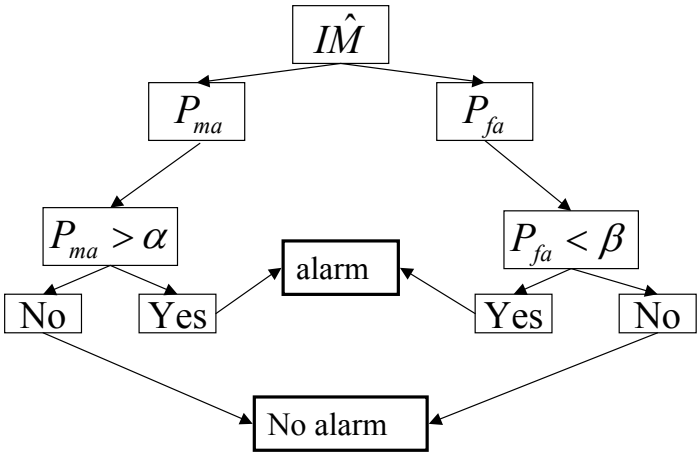

Figure 7. Decision making process based on probability of wrong decisions.

For the case of a missed alarm, the condition $P_{ma} > \alpha$ in Figure 7 and Eq. 51 give the time-varying expression for the warning threshold as follows:

$$P_{ma}(t) > \alpha \Leftrightarrow I\hat{M}(t) > a\left[1 - \frac{\sigma_{tot}(t)\Phi^{-1}(1-\alpha)}{a}\right] = c_{ma}(t)\cdot a \tag{52}$$

Therefore, the setting of the alarm based on the probability of a missed alarm becoming unacceptable occurs if $I\hat{M}(t) > c_{ma}(t)\cdot a$ where:

$$c_{ma}(t) = 1 - \frac{\sigma_{tot}(t)\cdot\Phi^{-1}(1-\alpha)}{a} \tag{53}$$

The alarm is also set if the probability of a false alarm falls below the tolerable level β and based on Eq. 49:

$$P_{fa}(t) < \beta \Leftrightarrow I\hat{M}(t) > a\left[1 - \frac{\sigma_{tot}(t)\Phi^{-1}(\beta)}{a}\right] = c_{fa}(t)\cdot a \tag{54}$$

that is, the alarm is set if $I\hat{M}(t) > c_{fa}(t)\cdot a$ where:

$$c_{fa}(t) = 1 - \frac{\sigma_{tot}(t)\cdot\Phi^{-1}(\beta)}{a} \tag{55}$$

Notice that if β<1-α, then $c_{ma}(t) < c_{fa}(t)$ and so the concern about missing an alarm will control the setting of the alarm; on the other hand, if β>1-α, then concern about causing a false alarm will control the setting of the alarm. Of course, making an alarm decision based on the exceedance of the predictor above the time-varying warning threshold is equivalent to monitoring the probability of $P_{fa}(t)$ and $P_{ma}(t)$ and raising the alarm based on exceedance of the tolerable level β and α, respectively.

It was pointed out in Section 4.3 that when the tolerable probabilities β and α to use during operation are based on cost-benefit considerations, they are related by: $\beta = 1 - \alpha$. Therefore, since both the alarm probabilities and their tolerable values sum up to one, the alarm probabilities will reach their critical thresholds at the same time, so one can choose to monitor either $P_{fa}(t)$ and $P_{ma}(t)$. Similarly, if the predictor $I\hat{M}(t)$ is monitored, the critical thresholds, $c_{ma}(t)a$ and $c_{fa}(t)a$, are equal and so are reached at the same time.

6. Application of EWS

6.1. Pre-installation analysis: Southern California

We suppose the future realization of a seismic EWS for the protection of facilities in Southern California and examine the question of the feasibility of applications of interest to the potential end-user. In particular, we address the question: How would an EWS perform during earthquakes that might occur in the area, viewed in terms of false and missed alarms? We can quantify the effectiveness of the EWS application by providing to the end-user the probabilities of wrong decisions to see whether they are acceptable and we can also set the warning threshold in order to match the user's requirements.

To illustrate the process, we choose a hazard function appropriate for the Los Angeles area to evaluate the probabilities of wrong decisions as a function of the warning threshold *c.a* and demonstrate that it can be set based on the tolerable level of probabilities of wrong decisions that come from a cost-benefit analysis. We assume that the critical threshold, *a*, has been selected by the user based on the EWS application of interest. The Virtual Seismologist method (Cua and Heaton 2004, Cua 2004) is chosen to give the earthquake predictive model (M_1 in Figure 1) and the attenuation model (M_2 in Figure 1) which in the VS method (Cua and Heaton 2002) is defined as:

$$IM = \log PGA = aM - b[R_1 + C(M)] - d\log[R_1 + C(M)] + e + \varepsilon \tag{56}$$

where M is the magnitude; R_1 depends on R which is the epicentral distance; $C(M)$ is a correction factor depending on magnitude. The residual term ε is a zero mean error term representing the prediction uncertainty and e is a constant error which includes station corrections; the parameters a, b, d, e are defined by the model's calibration by data fitting. The parameters a, b, d, e are estimated from data by Cua and Heaton for different soil types; for rock, they are: $a = 0.779$, $b = 2.55 \cdot 10^{-3}$, $d = 1.352$, $e = -0.645$ and ε is Gaussian (0, 0.243), i.e. with zero mean and standard deviation 0.243.

The intensity measure *IM* is the peak ground acceleration (PGA) on a $\log_{10}$ scale. The chosen hazard function for the Los Angeles area is shown in Figure 8 and it represents the mean rate of exceedance versus PGA in g units. The hazard function is fitted, as described previously, by minimizing the relative entropy in order to estimate the coefficient k_1 to describe the probability distribution for *IM* and a value of k_1=1.06 is obtained.

To simulate the behaviour of the EWS from *IM* to the predicted value, $\hat{IM}$, we need to know the total error associated with this process, as defined in the earlier uncertainty propagation analysis. It is assumed that the errors associated with the magnitude and location estimation and the attenuation model (Cua and Heaton, 2004) are described by:

- ε_M : Gaussian (0, 0.5)
- ε_R : ignored at this stage
- ε_{IM} : Gaussian (0, 0.243)

Therefore, the total error associated with the predicted $\hat{IM}$, as given by Eq. 8 and 9, is:

- ε_{tot} : Gaussian (0, 0.44)

The probabilities of false and missed alarms are evaluated based on Eq. 27 and 37 and are shown in Figures 9 and 10 as a function of the warning threshold factor *c* for different values of the critical threshold *a*. Notice that for P_{fa} in the approximate range of 0.05 to 0.4, the choice of *c* is insensitive to *a*. If it is false alarms that the user is more concerned about, the warning threshold can be set so that the tolerable level of probability of a false alarm is not exceeded. For example, if this tolerable level is P_{fa} = 0.4, then the warning threshold *ca* will be set equal to 2.22, as shown in Figure 11. Based on this warning threshold, the probability of a missed alarm that has to be accepted can then be evaluated as P_{ma} = 0.05, as shown in Figure 12 by the point on the curve corresponding to *ca*=2.22.

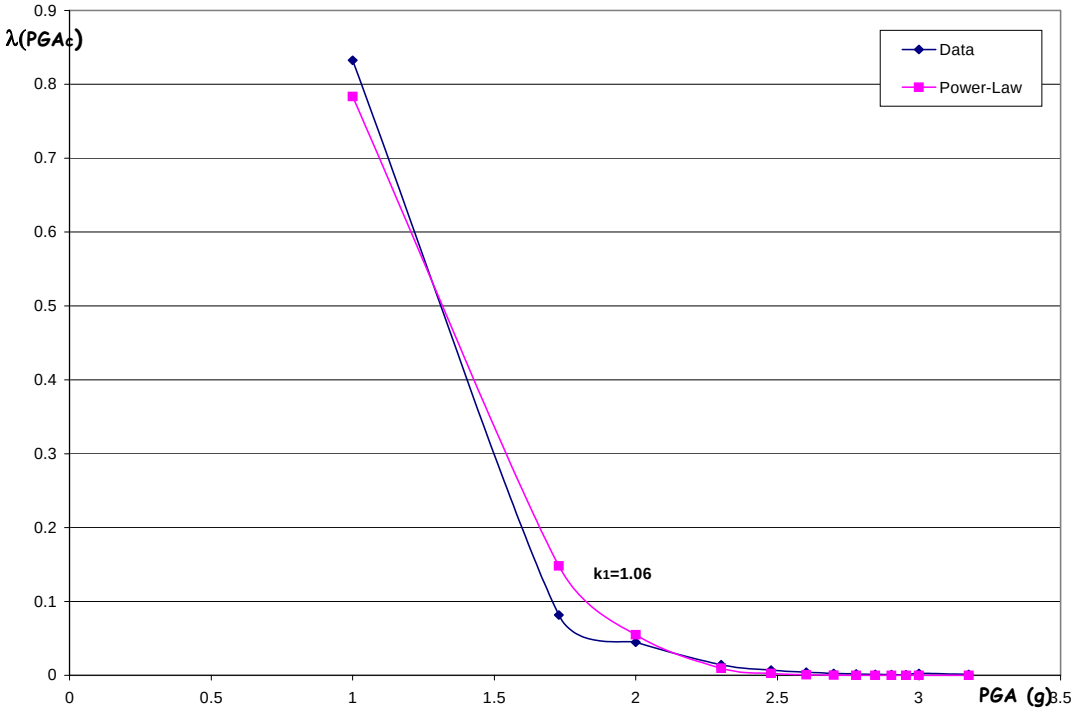

Figure 8. Fitting the hazard function for Los Angeles area with a power-law in PGA

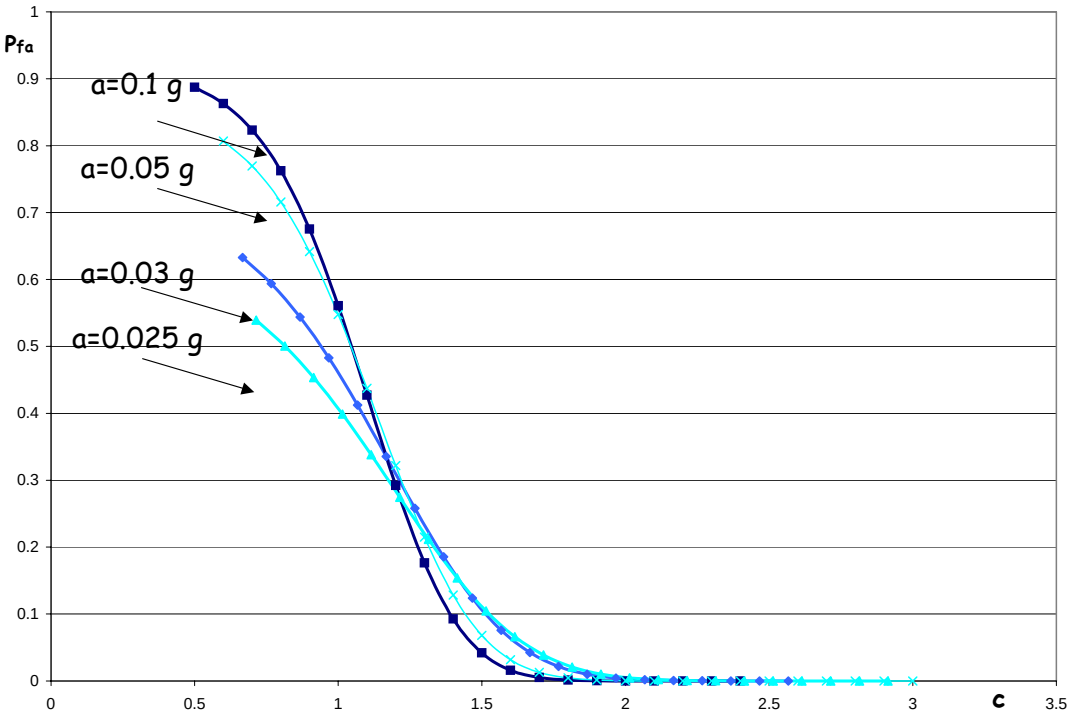

Figure 9. Probability of false alarm as a function of warning threshold factor *c* for different critical thresholds, *a*, expressed in g's.

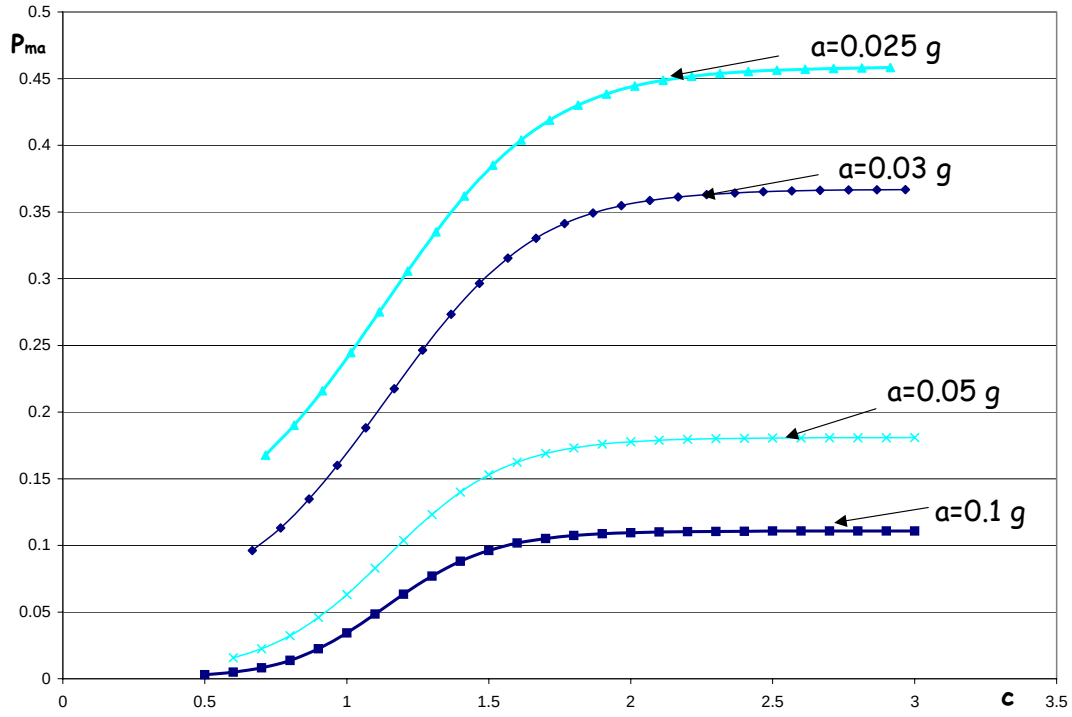

Figure 10. Probability of missed alarm as a function of warning threshold factor *c* for different critical thresholds, *a*, expressed in g's.

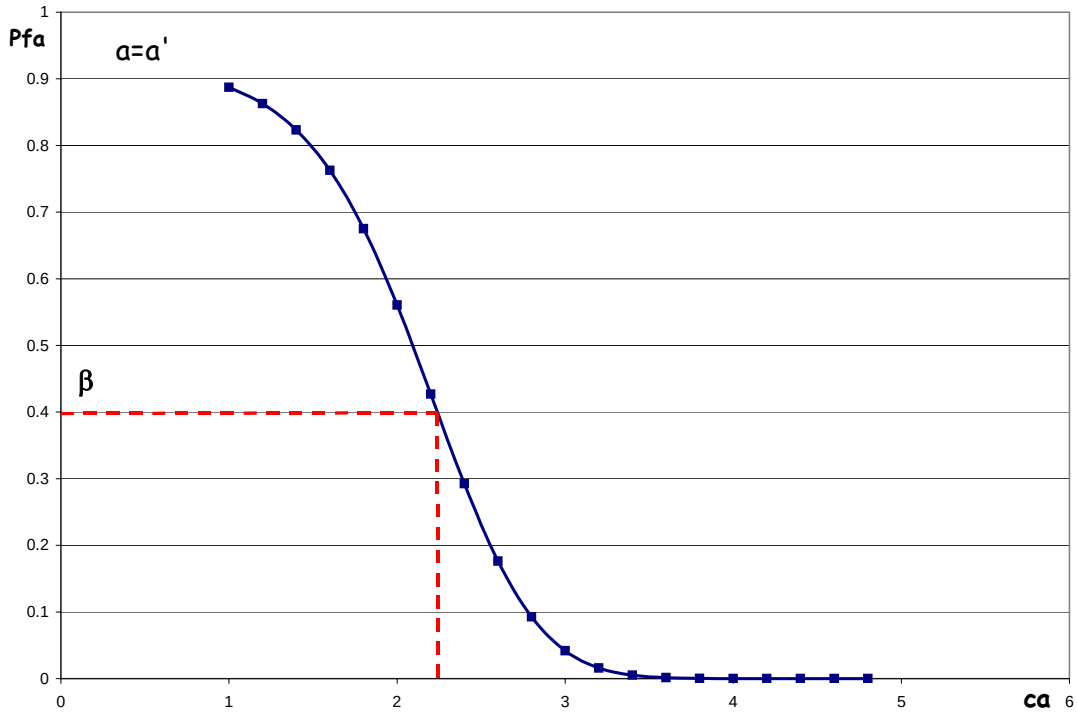

Figure 11. Probability of false alarm for a given critical threshold a′ as a function of the warning threshold.

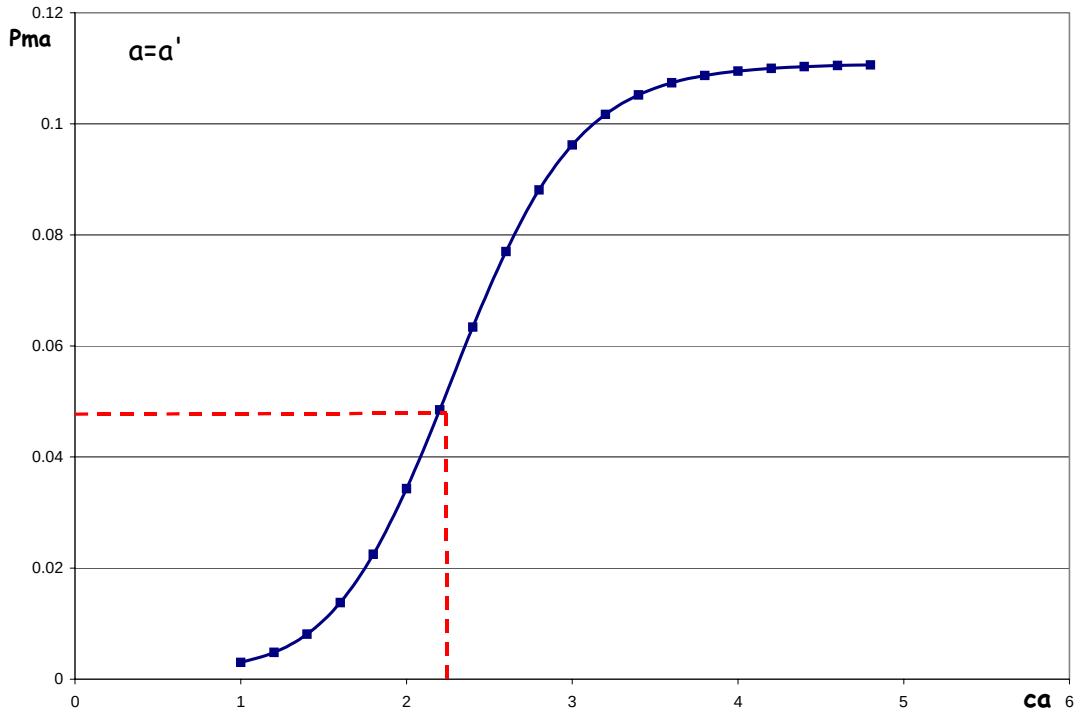

Figure 12. Probability of missed alarm for a given critical threshold a′ as a function of the warning threshold.

6.2. Yorba Linda Earthquake: *M*=4.75

On 3 September 2002, the Yorba Linda earthquake occurred in Orange County, California, with magnitude 4.75. The epicenter has been located at 33.9173^0 N and 117.7758^0 W with a depth of 12.92 Km. The area of the main shock is densely instrumented and the first station that was triggered by the event was the Serrano station at 9.9 Km from the epicenter. To simulate how the decision process would operate during a seismic event, the Virtual Seismologist magnitude and location estimates are used (Cua and Heaton 2004, Cua 2004).

The Virtual Seismologist method is based on continual Bayesian updating of the predictions of magnitude and location as an increasing amount of data arrives from newly triggered stations and from continued recording of data from the stations already triggered. Different prior information can be considered in the method, including the Gutenberg-Richter law for a prior probability

density (PDF) on magnitude, Voronoi cells to define the most likely locations, and recently observed seismicity to take into account any foreshocks that may have occurred in the area of interest in the 24 hours before the main shock.

As the first station is triggered, the Voronoi cell related to this station gives an area of possible locations since the cell is defined as all epicentral points that would give an event that is first recorded at the station. As a consequence, it is possible to define the prior PDF of most likely locations; the successive P arrivals that trigger other stations then provide additional information for the Bayesian updating of the prediction of epicentral distance. The most likely predictions of magnitude and location are those that maximize the joint posterior PDF given by:

$$p\left(M,R\,|\,\text{data}\right) \propto p(\text{data}\,|\,M,R)\cdot p(M,R) \tag{57}$$

The predictions from the Virtual Seismologist method for the magnitude and epicentral distance are available at 5, 10, 15, 20 and 50 seconds after the first station was triggered by the Yorba Linda earthquake. The epicentral distance prediction is considered time invariant, but the magnitude uncertainty is assumed to decrease as $1/\sqrt{N}$ where N is the number of stations contributing information (Cua and Heaton 2004). The updating of magnitude uncertainty is continued because the error associated with magnitude is more influential in the *IM* prediction process than the error associated with epicentral distance.

Using the temporal sequence of updated magnitude and location predictions given by Cua and Heaton (2004) for the Yorba Linda earthquake, we estimate the peak ground acceleration in $\log_{10}$ scale based on their attenuation relationship. The total uncertainty is updated every second as a function of the magnitude uncertainty and attenuation model uncertainty using Eq. 8 (neglecting location uncertainty, as mentioned above, because it is not as influential as the other two sources of uncertainty). The potential probabilities of wrong decisions are then evaluated at each second from Eq. 49 and 51. The results as a function of time are presented in Figure 13, which shows the PGA

prediction $\hat{IM}(t)$ (most probable value of IM = $\log_{10}$PGA at time t), the standard deviation of the error associated with the magnitude estimate and the potential probabilities of wrong decisions that were evaluated assuming the critical threshold for PGA is a=0.025g (corresponding to a=1.4 in $\log_{10}$ scale in cm\s\s).

These potential probabilities of wrong decisions may be used to make a decision during the event of whether to raise the alarm or do nothing, based on tolerable values of P_{fa} or P_{ma} derived from a cost-benefit analysis. For example, Figure 14 shows the plot of P_{fa} as a function of time and at about 28 seconds after the first station is triggered by the event, the tolerable value, $\beta = 0.4$, is reached and so the alarm would have then been raised (assuming that the minimum warning time for activation of the protective measure had not been reached before then).

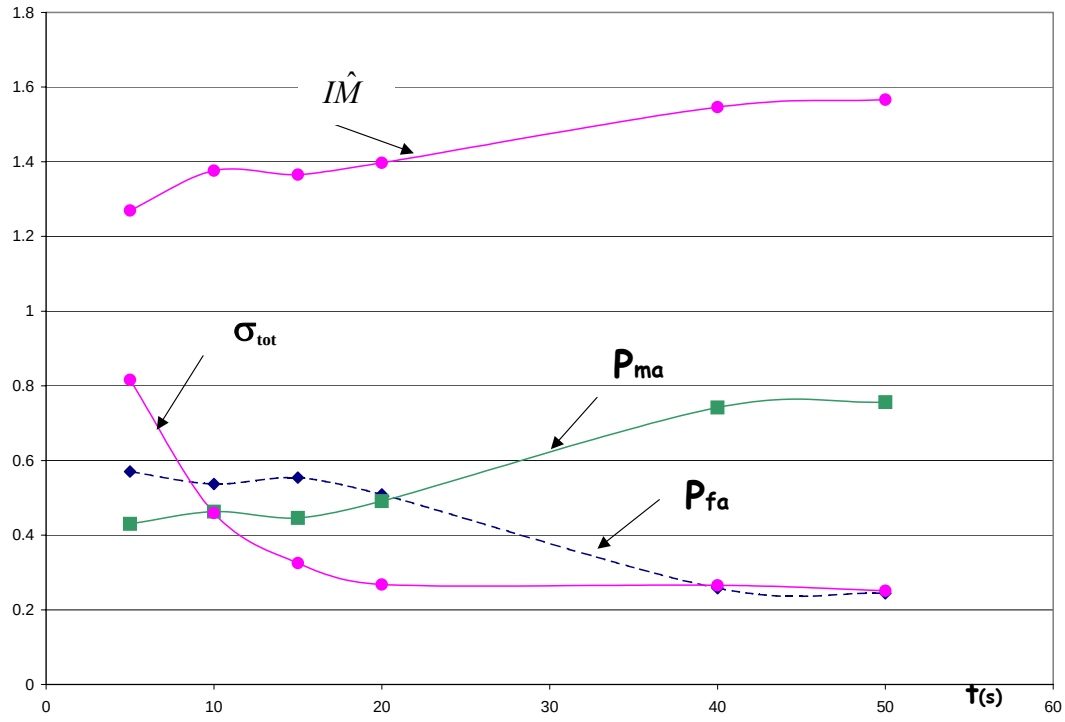

Figure 13. Yorba Linda 2002: Evolution of the prediction of IM, the standard deviation of magnitude prediction and the probabilities of wrong decisions (false and missed alarms) with time.

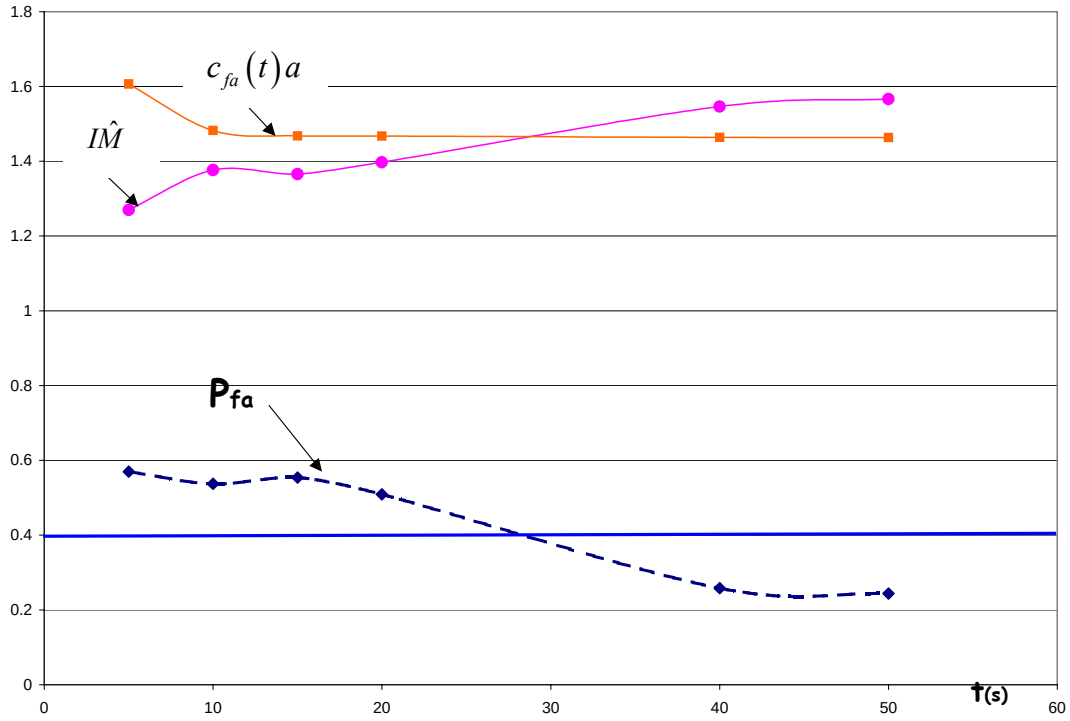

Figure 14. Yorba Linda 2002: Decision making based on tolerable probability of false alarm.

Alternatively, the threshold level $c_{fa}(t)$ in Eq. 55 can be determined and the alarm raised when $\hat{IM}(t)$ exceeds $c_{fa}(t)a$, which, of course, also occurs at about 28 seconds.

6.3. San Simeon Earthquake: *M*=6.5

On 22 December 2003, the San Simeon earthquake occurred on the central coast of California, with magnitude 6.5. The epicenter is located in 35.702^0 N and 121.08^0 W with a depth of 7 Km. The first station triggered by the event is the closest station to the epicenter, which is at Parkfield, about 57 Km from the epicenter. Unfortunately, the area in which the earthquake occurred is not densely instrumented and so the available data were not as extensive as for the 2002 Yorba Linda event described before. The predictions for magnitude and location are available from the Virtual Seismologist method (Cua and Heaton, 2004) at 3, 5.5, and 8 seconds after the first

station was triggered by the event. The epicentral distance variable is considered as time invariant at 57 Km based on the distance estimate from the first triggered station at Parkfield.

From Eq. 49 and 51, the potential probabilities of wrong decisions are evaluated and used as a tool for decision making during the event, assuming a=0.025g (1.4 in $\log_{10}$ scale in cm\s\s). The results are shown in Figures 15 and 16. Figure 16 shows that the alarm would have been raised about 6.3 seconds after the first station was triggered.

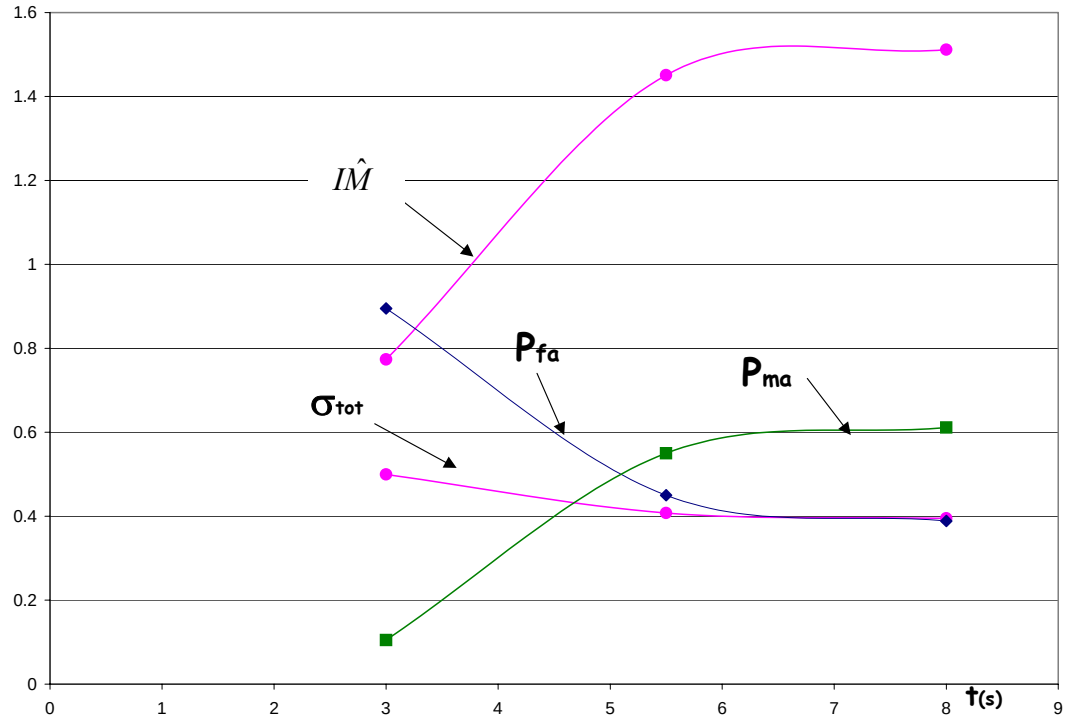

Figure 15. San Simeon 2003: Evolution of the prediction of *IM*, the standard deviation of magnitude prediction and the probabilities of wrong decisions (false and missed alarms) with time.

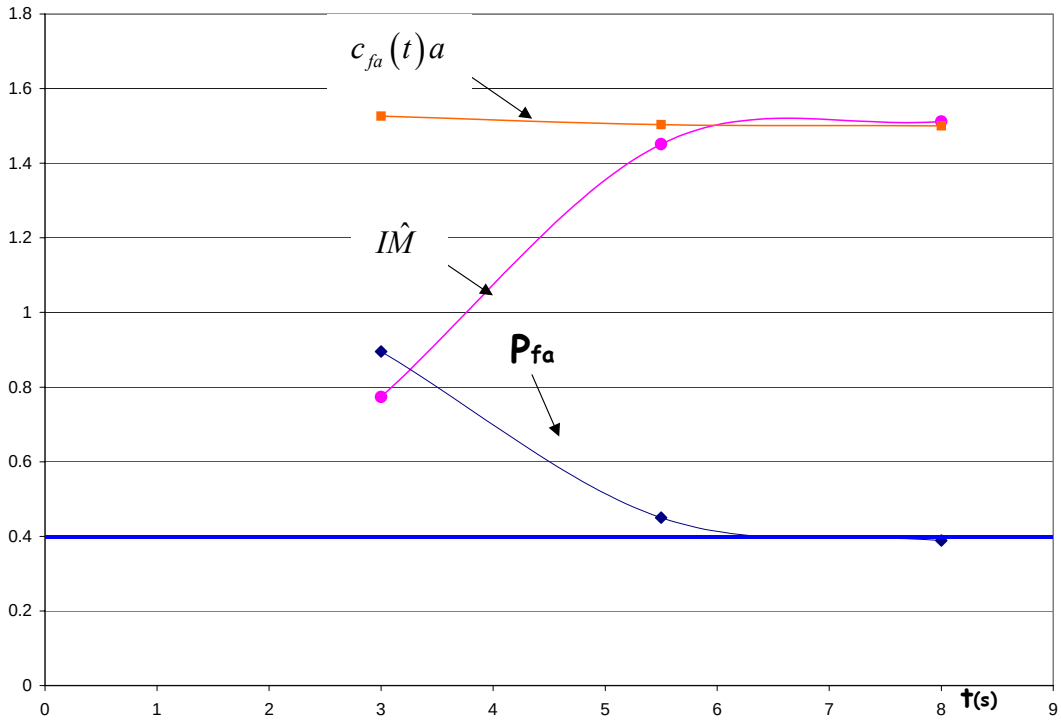

Figure 16. San Simeon 2003: Decision making based on tolerable probability of false alarm.

7. Concluding Remarks

This report presents a probabilistic methodology for EWS analysis and design to take into account the inherent uncertainties in making decisions based on predictions from limited seismic sensor data. The methodology provides a probabilistic description of the anticipated system performance (in terms of the probability of making wrong decisions) in a pre-installation feasibility assessment of an EWS. An example is shown for Southern California.

The performance of an EWS when operating in real-time is also explored and a methodology for deciding whether to raise the alarm or not is presented based on the probability of making wrong decisions. The methodology has been applied retro-actively to the Yorba Linda and San Simeon seismic events as illustrative examples.

The theory presented in this report using the ground motion intensity as the predictor could be readily extended to consider other quantities of interest that more closely represent the consequences of concern to the user, such as in terms of structural response (for example, interstory drift), non-structural and structural damage, safety or economic losses. These consequences can be predicted based on facility-specific loss estimation methods, such as the performance-based earthquake engineering (PBEE) framework (Porter *et al.* 2002, Porter *et al.* 2004).

The setting of the alarm during real-time operation of the EWS could then be based on monitoring the probabilities that specified engineering or economic parameters of interest would exceed their critical thresholds. The analysis is a natural extension of the previous theory; for example, to extend the probability of a missed alarm based on *IM* to that for an engineering demand parameter (*EDP*):

$$P_{ma}(t) = \mathrm{P}[EDP > e \mid \hat{IM}(t)] = \int_{-\infty}^{\infty} \mathrm{P}\left(EDP > e \mid IM\right) \mathrm{p}\left(IM \mid \hat{IM}(t)\right) dIM \tag{58}$$

where e is the critical threshold value of the EDP, $\mathrm{p}(IM \mid \hat{IM}(t))$, is a Gaussian PDF as before (see the integrand in Eq. 49) and $\mathrm{P}(EDP > e \mid IM)$ comes from a seismic vulnerability analysis for the facility (Porter *et al.* 2002, Porter *et al.* 2004).

Similarly, the probability of a missed alarm can be extended to damage or loss estimation:

$$P_{ma}(t) = \mathrm{P}[DV > d \mid \hat{IM}(t)] = \int_{-\infty}^{\infty} \int_{0}^{\infty} \mathrm{P}\left(DV > d \mid EDP\right) \mathrm{p}\left(EDP \mid IM\right) \mathrm{p}\left(IM \mid \hat{IM}(t)\right) dIM dEDP \tag{59}$$

where DV is a decision variable quantifying the damage or loss and d is the critical threshold value.

There are many theoretical and practical issues related to EWS assessment and operation that remain to be addressed. For example, what are the best indicators of EWS performance? What is required to demonstrate that EWS offers new value to owners and facility stakeholders? What type of information would decision makers like to know in a pre-installation phase in order to evaluate the benefits of applying EWS for seismic risk protection?

For further development of the methodology, it should be applied to real facilities where an EWS might produce the most value, such as applications to hospitals, schools, industrial plants, etc.

8. Appendix

8.1. Uncertainty propagation using Monte-Carlo simulation

In this section the goal is to test the analytical expression of the prediction error Eq. (8) shown in Section 2.3 by a Monte-Carlo simulation method and to lay out an alternative approach to uncertainty propagation when Eq. (8) is not applicable.

The prediction error, ε_{tot}, is calculated by propagating the single errors ε_M, ε_R and ε_{IM} through the output. The intensity measure represents the output of the prediction process provided by EWS as a function of magnitude and epicentral distance.

Magnitude and location in the uncertainty propagation process will be affected by errors, as shown in Figure 2 and which are modeled as described in the Section 2.2. Magnitude and source-to-site distance are described by a prior distribution representing the most likely values, for a given site of interest. The seismic rate is assumed to follow the Gutenberg-Richter law (1997):

$$\log_{10} N(M) = a - bM \tag{60}$$

or,

$$N(M) = 10^{a} \cdot 10^{-bM} \tag{61}$$

The value of *b* varies somewhat from area to area, but worldwide it seems to be around *b*=1. This value is assumed for *b* in this work, while *a*=6 is taken as representative of Sothern California, as confirmed by Cua and Heaton (2002). An interval of interest of magnitude values is defined for a better representation of the area seismicity, i.e. $[M_{min}, M_{max}]$. The probability distribution is normalized based on the interval of interest, imposing the condition that the integral of the distribution represented by Eq.(67) is equal to unity, so:

$$P\left[M \geq \hat{M} \mid M \in \left[M_{\min}, M_{\max} \right] \right] = \frac{10^{-b\hat{M}} - 10^{-bM_{\max}}}{10^{-bM_{\min}} - 10^{-bM_{\max}}} \qquad \hat{M} \in \left[M_{\min}, M_{\max} \right] \tag{62}$$

The normalized distribution function provides the cumulative distribution function from which randomly picked magnitude values may be choosen during Monte Carlo simulation:

$$P(\hat{M}) \underline{\underline{\Delta}} P\left[M \leq \hat{M} \mid M \in \left[M_{\min}, M_{\max} \right] \right] = \int_{M_{\min}}^{\hat{M}} p(M) dM = \frac{1}{\left(10^{-M_{\min}} - 10^{-M_{\max}} \right)} \left(10^{-M\min} - 10^{-\hat{M}} \right) \tag{63}$$

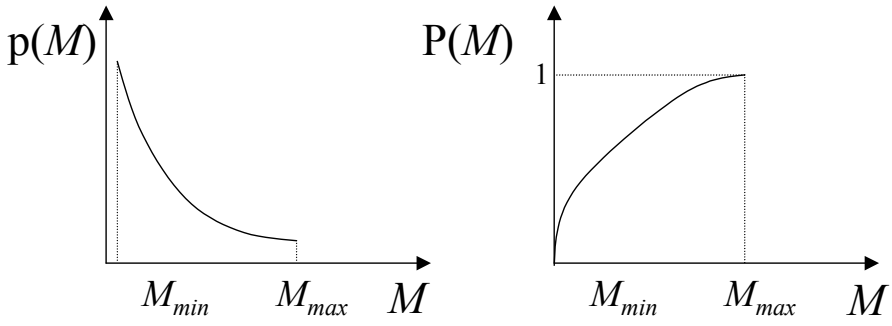

Figure 17. Probability distribution function p(*M*) and cumulative distribution function P(*M*) of magnitude, *M*.

Epicentral distance values are choosen based on a prior probability distribution function representing the most likely locations. One possibility for the epicentral distance distribution is based on considering the distribution of source locations to be equally likely in an circular area of radius R_{max} around the location of interest, so that:

$$p(R) = \frac{2R}{R_{\max}^2} \tag{64}$$

From the distribution of equally likely locations, the cumulative distribution for epicentral distances is derived, which can be used to randomly pick the values of epicentral distances during Monte Carlo simulation:

$$P(\hat{R}) \underline{\underline{\Delta}} P\left[R \leq \hat{R} \mid R \leq R_{\max} \right] = \int_{0}^{\hat{R}} \frac{2R}{R_{\max}^2} dR = \frac{R^2}{R_{\max}^2} \tag{65}$$

In the Monte-Carlo analysis, values of magnitude and locations representing the actual values M and R are randomly picked from the corresponding cumulative distribution functions.

Considering that EWS estimates of magnitude and distance, $\hat{M}$ and $\hat{R}$, are affected by errors, the predictions are created by adding the related errors to the real values of M and R.

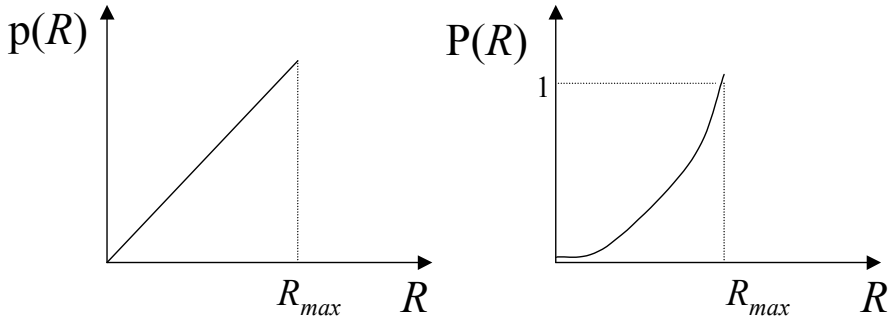

Figure 18. Probability distribution function p(R) and cumulative distribution function P(R) of epicentral distance, R assuming locations equally likely in an area of radius Rmax around the site of interest.

The errors of magnitude and epicentral distance estimates are obtained by randomly picking values from the distributions of errors ε_M and ε_R. The estimates of magnitude and epicentral distance are therefore:

$$\hat{M} = M + \varepsilon_M \tag{66}$$

$$\hat{R} = R + \varepsilon_R \tag{67}$$

As noted previously, the prediction errors, ε_M, ε_R and ε_{IM}, are modeled as Gaussian distributions (choosing $\log_e R$ as basic Gaussian variable).

The predicted intensity measure $\hat{IM}$ is estimated from the ground motion attenuation model, as a function of the simulated $\hat{M}$ and $\hat{R}$. The error related to the attenuation model is considered for each Monte-Carlo cycle by randomly choosing a value from a Gaussian distribution with zero mean and a standard deviation dependent on the attenuation model used. As a result, $\hat{IM}$ is a function of the values M, R and the uncertainties ε_M, ε_R and ε_{IM}:

$$\hat{IM} = f(\hat{M}, \hat{R}) + \varepsilon_{IM} = f(M + \varepsilon_M, R + \varepsilon_R) + \varepsilon_{IM} \tag{68}$$

where the function *f* represents the attenuation model. The actual intensity measure*, IM*, is:

$$IM = f(M, R) \tag{69}$$

IM is evaluated for each value of magnitude and location, *M* and *R*, extracted from the cumulative distributions during the Monte-Carlo simulation. The prediction error associated with the ground motion parameter is given by the difference between the predicted intensity measure and the actual value.

The process for uncertainty propagation by Monte-Carlo simulation is shown in Figure 19. The results, ε_{tot}, obtained from the Monte-Carlo simulations are then plotted as a histogram and fitted with a Gaussian distribution, as shown in Figure 20. The case considered is where the error ε_M associated with the magnitude prediction is modeled as a Gaussian distribution with zero mean and 0.5 standard deviation, and the error ε_{IM} related to the attenuation model is modeled as a Gaussian distribution with zero mean and 0.3 standard deviation (Cua and Heaton, 2004). The total error follows a Gaussian distribution with zero mean and standard deviation equal to 0.44 (Figure 20), which is consistent with the considerations in Eq. (8).

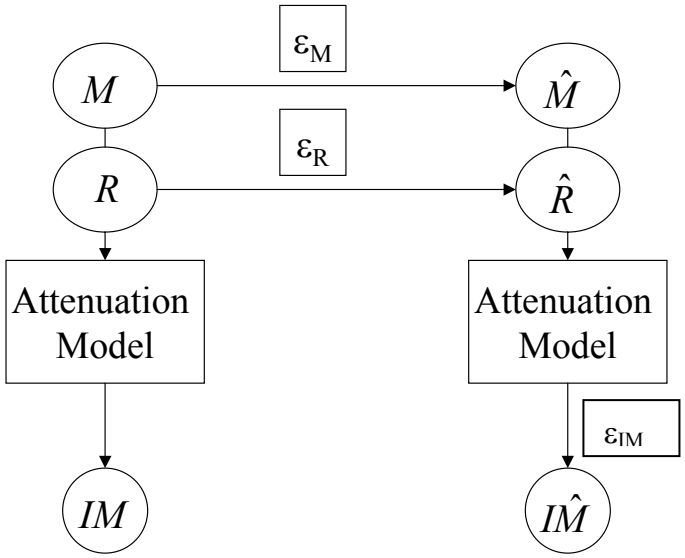

Figure 19. Uncertainty progation process with Monte-Carlo method.

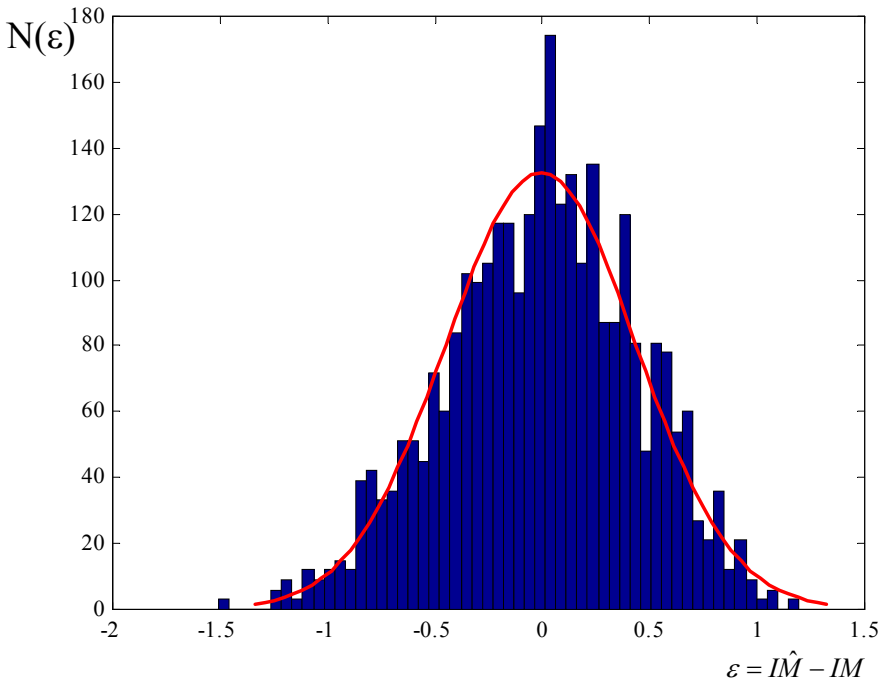

Figure 20. Probability distribution function of the error related to the prediction. The error is given by the difference between the predicted intensity measure and the actual value.

9. References

Allen, R.M. and Kanamori, H., The Potential for Earthquake Early Warning in Southern California, *Science*, 300: 786-789, 2003.

Allen, R.M., Rapid Magnitude Determination for Earthquake Early Warning, Proceedings of Workshop on Multidisciplinary Approach to Seismic Risk Problems," Sant'Angelo dei Lombardi, September 22, 2003.

Bates, S., Cullen A., and Raftery, A., Bayesian Uncertainty Assessment in Multi-compartment Deterministic Simulation Models for Environmental Risk Assessment, *Environmetrics*, 14: 355-371, 2003.

Cua, G. and Heaton, T., Illustrating the Virtual Seismologist (VS) Method for Seismic Early Warning on the 3 September 2002 M=4.75 Yorba Linda, California Earthquake, 2004 SCEC Annual Meeting Proceedings and Abstracts, Volume XIV, 2004.

Cua, G. and Heaton, T., Characterizing Average Properties of Southern California Ground Motion Envelopes, 2004 SCEC Annual Meeting Proceedings and Abstracts, Volume XIV, 2004.

Cua, G., Creating the Virtual Seismologist: developments in ground motion characterization and seismic early warning, PhD Thesis in Civil Engineering, California Institute of Technology, Pasadena, December 2004: http://resolver.caltech.edu/CaltechETD:etd-02092005-125601

Grasso V.F., Iervolino I., Occhiuzzi A., Manfredi G., Critical Issues of Seismic Early Warning Systems for Structural Control, Proceedings of 9th International Conference on Structural Safety and Reliability, Rome, Italy, June 2005.

Kanda, K., Kobori, T., Ikeda, Y. and Koshida, H., The Development of a Pre-arrival Transmission System for Earthquake Information Applied to Seismic Response Controlled Structures, Proceedings of 1st World Conference on Structural Control, 2, IASC, California, USA, 1994.

Kramer, S.L., Geotechnical Earthquake Engineering, Prentice-Hall, 1996.

Lee, W.H.K. and Espinosa-Aranda, J.M., Earthquake Early Warning Systems: Current Status and Perspectives, Proceedings of International Conference on Early Warning Systems for Natural Disaster Reduction, 409-423, 1998.

Occhiuzzi A., Grasso, V.F. and Manfredi, G., Early Warning Systems from a Structural Control Perspective, Proceedings 3rd European Conference on Structural Control, Vienna University of Technology, Austria, July 2004.

Porter, K.A., J.L. Beck and R.V. Shaikhutdinov, Sensitivity of Building Loss Estimates to Major Uncertain Variables, *Earthquake Spectra*, 18, 719-743, November 2002.

Porter, K.A., J.L. Beck, R.V. Shaikhutdinov, S.K. Au, K. Mizukoshi, M. Miyamura, H. Ishida, T. Moroi, Y. Tsukada and M. Masuda, Effect of Seismic Risk on Lifetime Property Values, *Earthquake Spectra,* 20, 1211-1237, November 2004.

Saita J., Nakamura Y., UrEDAS: The Early Warning System for Mitigation of Disasters caused by Earthquakes and Tsunamis. Proceedings of International Conference on Early Warning Systems for Natural Disaster Reduction, EWC98, 453-460, 1998.

Seismological Research Letters, Issue on Ground Motion Attenuation Models, 68: (1), 1997.

Wald, A., Sequential Analysis**,** J. Wiley & Sons, New York, and Chapman & Hall, London, 1947.

Wieland, M., Griesser, L., and Kuendig, C., Seismic Early Warning System for a Nuclear Power Plant. Proceedings of 12th World Conference on Earthquake Engineering, Auckland, New Zealand, 2000.

Wieland M., Earthquake Alarm, Rapid Response and Early Warning Systems: Low Cost Systems for Seismic Risk Reduction. Proceedings of International Workshop on Disaster Reduction, Reston, Virginia, U.S., August, 2001.